Nuclear Magnetic Resonance Saturation and Rotary Saturation in Solids*

ALFRED G. REDFIELD†
Division of Applied Science, Harvard University, Cambridge, Massachusetts
(Received March 14, 1955)

Nuclear spin-lattice relaxation times of Al^{27} in pure Al and Cu^{63} in annealed pure Cu have been measured with a nuclear induction spectrometer, by the method of saturation. The experimental values of T_1 are 4.1±0.8 milliseconds for Al^{27} and 3.0±0.6 milliseconds for Cu^{63}, in reasonable agreement with theory.

The dispersion mode of the nuclear resonance was also observed, and it was found that χ' (the real part of the rf susceptibility) does not saturate at the same level as the absorption, χ'', but remains roughly constant out to a radio-frequency field intensity of about 2 gauss. Both χ' and χ'' become narrower and nearly Lorentzian in shape above saturation. When the dc magnetic field modulation is increased from 14 to 41 cps the phase of the dispersion signal lags behind the modulation, presumably because the modulation period is then comparable to T_1. Large dispersion signals above saturation have also been observed for the Na^{23} resonance in NaCl.

This behavior of the dispersion mode is in conflict with the predictions of Bloembergen, Purcell, and Pound and of the Bloch equations. The validity of these theories is re-examined, and it is concluded that although they are applicable to nuclear resonance in liquids and gases, and to solids at small rf intensities, they contain incorrect assumptions as applied to solids at high rf power levels. The theory of Bloembergen, Purcell, and Pound is based on an assumption equivalent to that of a spin temperature. It is shown that the spin state cannot be strictly described by a spin temperature because the phases of the spin quantum states are not incoherent, as required by the temperature concept. The transverse decay of the nuclear magnetization predicted by the Bloch equations is shown to be partially forbidden by energy and entropy considerations if a large rf field at the resonance frequency is continuously applied to the solid.

A theory is developed which is applicable only to solids at rf magnetic field intensities well above the saturation level and which is in reasonable agreement with the experimental observations. The Hamiltonian is transformed to a coordinate system rotating at the frequency of the rf field. The resulting time-dependent parts of the spin-spin interaction are nonsecular perturbations on the time-independent part, and can therefore be ignored. Statistical mechanics is applied to the remaining stationary spin Hamiltonian; specifically it is assumed that the spin system is in its most probable macrostate (a canonical distribution of quantum states) with respect to the transformed spin Hamiltonian. This assumption is justified because the transformed spin Hamiltonian is effectively time independent and the spin-lattice interaction is small, and it is analogous to assumptions basic to classical acoustics and fluid mechanics. The spin-lattice interaction merely determines the expectation value of the transformed spin Hamiltonian, which can be readily calculated under the assumption that the expectation value of the spin angular momentum of each spin is relaxed independently to its thermal equilibrium value by the lattice in time T_1. Both fast and slow modulation of the dc magnetic field can be treated.

"Rotary saturation" is observed by applying an audio-frequency magnetic field to the sample in the dc field direction while observing the dispersion derivative at resonance with a large rf field H_1. When the audio-frequency approaches γH_1 the dispersion signal decreases and goes through a minimum. The effect is easily treated theoretically in solids, liquids and gases by using a rotating coordinate system, and is a rotary analogue of ordinary saturation. It is a convenient method for calibrating rf magnetic fields and appears potentially capable of providing useful information on the solid state. Experimental data on rotary saturation are presented and discussed.

I. INTRODUCTION

THIS paper reports an experimental and theoretical study of nuclear magnetic resonance in solids at high rf magnetic field intensity. Metallic copper and aluminum were experimentally investigated, and the original objective of this work was to obtain nuclear spin-lattice relaxation times in these metals for comparison with the observed[1] Knight shifts[2] and the theory of Korringa,[3] which relates the relaxation times and Knight shifts to the electronic structure of the metals. The spin lattice relaxation times were measured by the method of saturation.

In the course of these measurements it was found that the dispersion mode of the nuclear resonance signal behaves in a way which is in conflict with the existing theories[4-6] of magnetic resonance saturation. As a re-

sult, the validity of these theories as applied to solids was re-examined, and a theory was developed along somewhat different lines which appears to agree with experiment for rf magnetic field intensities well above the saturation level. This theory also suggested the possibility of observing an effect which we call "rotary saturation," analogous to ordinary saturation but taking place in the effective field of a rotating coordinate system.

II. SATURATION DATA AND DISCUSSION

The experimental apparatus was a nuclear induction spectrometer[4] similar to those previously built by Weaver[7] and by Jeffries.[8] The details will be described elsewhere. The most important new feature of this equipment was a suitable calibrating circuit, permitting relative measurements of rf nuclear susceptibility to be made independent of receiver gain, rf level, and other variables. The output of this spectrometer yields the

[1] H. S. Gutowski and B. R. McGarvey, J. Chem. Phys. 20, 1472 (1952).
[2] W. D. Knight, Phys. Rev. 76, 1259 (1949).
[3] J. Korringa, Physica 16, 601 (1950).
[4] F. Bloch, Phys. Rev. 70, 460 (1946).
[5] Bloembergen, Purcell, and Pound, Phys. Rev. 73, 679 (1948) (henceforth referred to as BPP).
[6] A. M. Portis, Phys. Rev. 91, 1071 (1953).
[7] H. E. Weaver, Phys. Rev. 89, 923 (1953).
[8] C. D. Jeffries (private communication to Professor Bloembergen). We are indebted to Professor Jeffries for information on his spectrograph.

derivatives of the real and imaginary susceptibilities[9] χ' and χ''. The rf intensity was determined to an accuracy of better than 5 percent using the method of rotary saturation described below. All data were obtained at room temperature.

Powdered samples of pure aluminum and annealed pure copper were prepared as described by Bloembergen and Rowland.[10] In these samples, electric quadrupole effects are relatively small and can evidently be neglected.[10,11]

The relative absorption at resonance was measured by integrating the recorded absorption signal. The absorption data are plotted in Fig. 1, for an rf frequency of 7.6 Mc/sec and a magnetic field modulation frequency of 14 cps. In both aluminum and copper the absorption appears to follow the expected[4-6] dependence on rf field intensity for a system of dipolar coupled spins:

$$\chi''(\nu_0,H_1)=\chi''(\nu_0,0)[1+\tfrac{1}{2}\gamma^2H_1^2T_1g(\nu_0)]^{-1}, \quad (1)$$

where $\chi''(\nu_0,H_1)$ is the imaginary part of the nuclear magnetic susceptibility, $g(\nu)$ is the shape function of the unsaturated resonance, ν_0 is the resonance frequency, and H_1 is the magnitude of the rotating rf field.[12]

The shape function $g(\nu)$ is normalized with respect to integration over frequency:

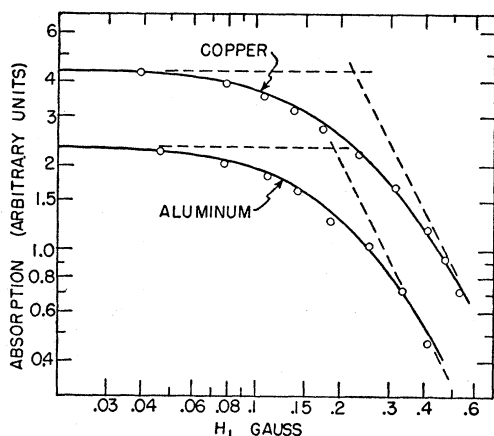$$\int_0^\infty g(\nu)d\nu=1. \quad (2)$$

FIG. 1. Relative absorption at resonance $\chi''(\nu_0)$ as a function of rf field intensity. The units of $\chi''(\nu_0)$ are not the same for aluminum and copper in this figure.

[9] Throughout this paper we use χ to denote the $x-x$ component of the complex susceptibility tensor defined by $M=\mathrm{Re}[(\chi'+i\chi'')H\exp i\omega t]$, where M is the oscillatory magnetization produced by the rf field $H\cos\omega t$. The experimentally observed quantity is the off-diagonal element χ_{yx} which is equal to $\pm i\chi_{xx}$ for a spin system in a large dc magnetic field.

[10] N. Bloembergen and T. J. Rowland, Acta Metallurgica 1, 731 (1953).

[11] T. J. Rowland, Acta Metallurgica (to be published).

[12] Throughout this paper the rf field intensity, denoted by H_1, will be the amplitude of one of the circularly polarized modes which comprise the applied linearly polarized rf field of peak amplitude $2H_1$.

Values of $g(\nu_0)$ were obtained by integrating the integrated absorption signal, and T_1 was obtained from the data of Fig. 1 using Eq. (1). As will be discussed below, there is some question about the correctness of (1), but it is believed that values of T_1 obtained in this way are reasonably accurate.

Korringa[3] has developed the theory of nuclear magnetic relaxation and the Knight shift in metals. His theory has been discussed by Bloembergen and Rowland[10] and by Holcomb and Norberg.[13] Korringa obtains the result

$$T_1^{-1}=\frac{4\pi kT}{\hbar}\rho^+(\epsilon_0)\rho^-(\epsilon_0)\left[\frac{8\pi v_0 g\beta^2 P_F}{3}\right]^2, \quad (3)$$

where v_0 is the atomic volume, $\rho^\pm(\epsilon_0)$ are the densities of electronic states per unit volume per unit energy range for spins up and down respectively, evaluated at the Fermi level, P_F is the electronic probability density evaluated at the nucleus for an electron in the Fermi surface (assuming that the electronic wave function is normalized to unity over the atomic volume v_0), g is the nuclear g-factor $\mu_N/I\beta$, and β is the Bohr magneton. In deriving this equation the effect of electronic correlations and of possible P-character (asymmetry) in the electronic wave function has been neglected.[10] The latter assumption is approximately justified unless the P-character part of the electronic wave function is much greater than the S-character part.

Korringa also obtained a value for the Knight shift which can be written

$$(\Delta H/H_0)^2=\hbar/\pi kTg^2T_1, \quad (4)$$

where T_1 is given by (3), ΔH is the Knight shift in gauss, and H_0 is the applied magnetic field in gauss. The effect of electronic correlations is also neglected in this expression.

In Table I are listed experimental values of $g(\nu_0)$, T_1 and $\Delta H/H_0$, together with the theoretical values of T_1 obtained from Eq. (4) and the experimental values of $\Delta H/H_0$. Also included in Table I are the values of $v_0 P_F m^*/m$ obtained from Eq. (3) and the experimental T_1 values, assuming the electrons in the metal can be treated as a Fermi gas with $m^*=m$, and with one electron per atom. The quantity $v_0 P_F$ is the magnitude of the square of the wave function at the nucleus for an average electron at the Fermi level, relative to that predicted by the plane-wave approximation. Since relaxation effects due to possible P-character in the electronic wave function have been neglected in (3), the values of $v_0 P_F m^*/m$ given in Table I must be regarded as upper limits.

The discrepancy between the theoretical and experimental values of T_1 in copper is probably due to electronic correlation effects. According to Pines,[14] it is

[13] D. F. Holcomb and R. E. Norberg, Phys. Rev. 98, 1074 (1955).

[14] D. Pines (private communication). We wish to thank Dr. Pines for permission to quote him.

reasonable to assume that correlations affect T_1 only by changing the density of electronic states from $\rho^{\pm}(\epsilon_0)$ to ρ_c, where ρ_c is the actual density of states of the correlated electron gas. The corresponding change in T_1 is $[\rho^{\pm}(\epsilon_0)/\rho_c]^2$, which Pines estimates to be approximately unity in both copper and aluminum. Correlations will also affect the Knight shift by increasing the paramagnetic susceptibility of the electron gas from χ_p, its uncorrelated value, to χ_{pc}. The corresponding increase in the Knight shift is χ_{pc}/χ_p, which Pines estimates to be 1.35 for copper and 1.3 for aluminum. If we apply these corrections to (4), we get theoretical T_1 values of 4 milliseconds for copper and 8.5 milliseconds for aluminum. The agreement with experiment is good for copper and poor for aluminum. The remaining discrepancy in aluminum may be due to the effect of possible P-character of the electronic wave function, the existence of which is likely because the valence electron of an aluminum atom is a P-electron. The data in both aluminum and copper are in poor agreement with extrapolation from measurements[15,16] of T_1 at low temperatures.

TABLE I. Experimental values of the inverse line width, relaxation time, and Knight shift, and related theoretical predictions of the relaxation time and mean electronic probability density at the nucleus.

	Aluminum	Copper
$g(\nu_0)$ milliseconds	0.212 ± 0.02[a]	0.228 ± 0.02[b]
T_1 milliseconds[b]	4.1 ± 0.8	3.0 ± 0.6
$\Delta H/H_0$[c]	0.237×10^{-2}	0.161×10^{-2}
T_1 milliseconds (theoretical)	5.06	2.26
$(m^*/m)v_0 P_F$[b]	250	260

[a] T. J. Rowland (private communication).
[b] Present research.
[c] See reference 1.

The derivatives of the absorption and dispersion obtained in aluminum at various rf intensities are shown in Fig. 2. The resonance curves observed in copper are similar at high rf levels, but more nearly Gaussian at low rf levels.

The important feature of these curves is the fact that the dispersion does not saturate at the same level as the absorption, but remains roughly constant out to a level of several gauss rf. As will be discussed below, this behavior is in strong conflict with the existing theories of magnetic resonance saturation in solids, which predict that both the absorption and dispersion should decrease (near resonance) at the same level, according to (1). Portis[6] has observed similar nonsaturation of the dispersion in the case of paramagnetic resonance in F-centers, but the saturation behavior of the absorption was different. The theory developed by Portis for the case of F-centers is not applicable here, because the different nuclei are tightly coupled by the dipolar interaction.

[15] N. J. Poulis, Physica 16, 373 (1950).
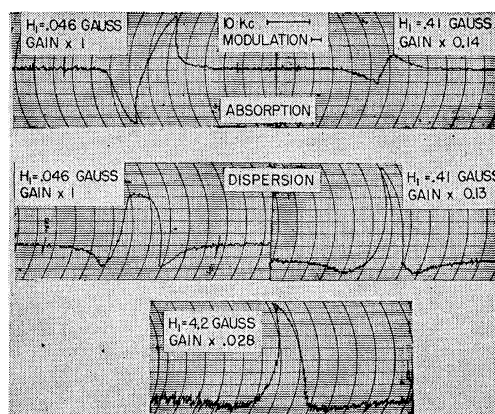[16] N. Bloembergen, Physica 15, 588 (1949).

FIG. 2. Absorption and dispersion signals in pure aluminum at various rf power levels. The modulation was 14~ in phase with the lock-in detector and the resonance frequency was about 7.6 megacycles per second.

The absorption line becomes narrower above saturation, as previously reported by Abell and Knight,[17] and similar narrowing occurs in the derivative of the dispersion. This is also in conflict with theory, which predicts that the absorption and dispersion curves should both broaden upon saturation.

The audio phase of the signal at the output of the receiver was not the same as the phase of the modulation applied to the dc magnetic field H_0. In the limit of small modulation frequency, the nuclear resonance signal and the modulation appear to be in phase, and the output of the lock-in amplifier probably represents the true derivative of the absorption and dispersion. As the modulation frequency is increased, however, the nuclear resonance signal lags behind the modulation. The apparent derivative of the absorption or dispersion, as indicated by the lock-in detector, is then not the true derivative, and a resonance signal can also be observed by changing the lock-in detector phase to 90° with respect to its normal setting. This phenomenon is evidently not directly related to the nonsaturation of the dispersion mode noted in the paragraph immediately above. The phase lag of the resonance signal relative to the modulation is evidently a consequence of the fact that the modulation period is comparable to T_1. A similar phase lag can be observed in systems obeying the Bloch equations, as experimentally and theoretically investigated by Halbach.[18]

In Figs. 3 and 4 are shown the apparent dispersion derivatives at resonance in copper and aluminum, observed with two different modulation frequencies and with the lock-in detector adjusted to detect signals either in phase or in quadrature with the modulation. The in-phase data obtained at 14 cps are apparently very nearly what would be observed in the limit of low modulation frequency, ("slow passage") and therefore

[17] D. F. Abell and W. D. Knight, Phys. Rev. 93, 940 (1954).
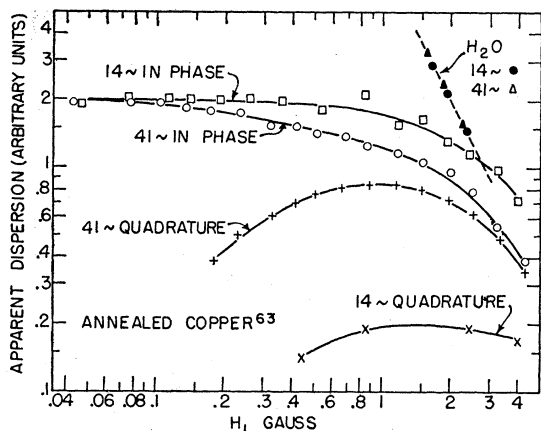[18] K. Halbach, Helv. Phys. Acta 27, 259 (1954).

FIG. 3. Apparent relative dispersion derivatives at resonance per resonating nucleus as a function of rf power, for Cu[63] in annealed copper and protons in impure water. The modulation frequency and phase relative to the lock-in detector are as marked.

nearly correctly represent the behavior of the true derivative of the steady-state dispersion.

For purposes of calibration and comparison, Figs. 3 and 4 also include the derivative of the dispersion at resonance of protons in water at the same frequency (thus at a smaller magnetic field) as that used to obtain the aluminum and copper data. The water was heavily doped with paramagnetic impurity (manganese sulfate) and the relaxation time of the protons was of the order of $\frac{1}{5}$ millisecond. The Bloch equations predict that well above saturation the derivative of the real part of the nuclear susceptibility of such a sample should be (at resonance)

$$\frac{\partial \chi'}{\partial H_0} = \frac{\chi_0 H_0 T_{2H}}{2 H_1^2 T_{1H}}, \tag{6}$$

where χ_0 is the proton contribution to the static nuclear susceptibility and T_{2H} and T_{1H} are the transverse and longitudinal relaxation times[4] for the protons in the sample. The water and metal samples occupied nearly the same volume in the nuclear induction head, so that no geometrical correction is necessary for comparison.

The quantity plotted in Figs. 3 and 4 is the output of the lock-in detector divided by the product of the rf input level to the nuclear induction head, the modulation amplitude, the total number of resonated nuclei in the sample, the Q-factor of the receiver coil in the nuclear induction head, and the over-all gain of the receiver and lock-in detector. Of these corrections, the first and the last two were given automatically by the calibration circuit. In the limit of low modulation frequency the quantity plotted in Figs. 3 and 4 should be the relative contribution per nucleus to the rf susceptibility derivative at resonance. The accuracy of these data is thought to be better than ± 20 percent.

Apparently these effects are not limited to metals, but are characteristic of solids in general, well below their melting points. In insulating solids the observed dis-

persion signals are in most cases different from what they are in metals, because the relaxation time is likely to be longer than the period of the dc magnetic field modulation. In Fig. 5 are shown dispersion signals obtained from two NaCl samples of different purity. In the impure NaCl, the relaxation time is thought to be long compared to the modulation period and short compared to the several minutes required to pass through resonance. A similar dispersion curve can be obtained from distilled water at high rf levels, as discussed by Halbach.[18] In the Harshaw NaCl the relaxation time is clearly of the order of the time (about one minute) taken to sweep through the resonance, as indicated by the asymmetry and hysteresis in the observed dispersion signal.

We conclude this section by noting that the shape and magnitude of the observed dispersion signals in both metals and insulators can be accounted for by the assumption that in the limit of large H_1 the Bloch equations hold with $T_1 \simeq T_2$, rather than $T_2 = \frac{1}{2} g(\nu_0)$ as is required to yield the correct line width below saturation. This assumption will be more or less justified in the next section, and the resulting predictions and comparison with experiment will be discussed there and in Sec. IV.

III. THEORY

A. Previous Saturation Theories

We now discuss the previous theories[4-6] of magnetic resonance saturation which lead to incorrect predictions of the magnitude of the dispersion at high rf field intensities in solids. Throughout this paper we are concerned with solids in which the nuclei can be regarded as fixed in their lattice positions, and we neglect diffusion and lattice vibrations. This is justified only well below the melting point.
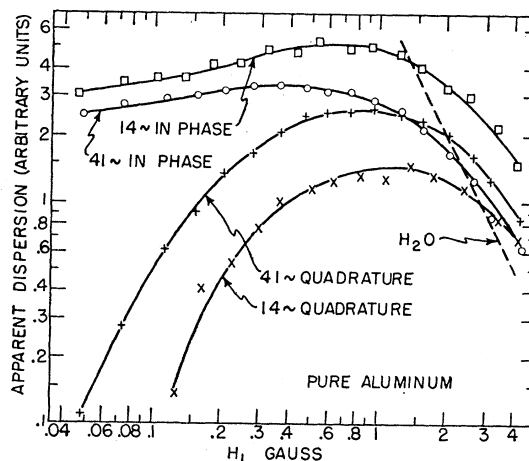

FIG. 4. Apparent relative dispersion derivatives at resonance per resonating nucleus as a function of rf power, for Al[27] in pure aluminum and protons in impure water. The units of $N^{-1} \partial \chi' / \partial H_0$ are the same as in Fig. 2 and to avoid confusion the actual H_2O data are omitted and only the dotted line through the H_2O points of Fig. 2 is included.

The theory developed by BPP[5] is the simpler of the two approaches to saturation in magnetic resonance, and is based on three assumptions. The first of these is that the effect of the spin-lattice interaction is to relax the spins to their equilibrium state in a time T_1. This is evidently correct, at least to a good approximation, in most cases. The second assumption is that the spins interact strongly with one another, so that energy absorbed at one frequency of the dipolar broadened resonance line is quickly transferred to all the spins, whether or not they are in a local field exactly corresponding to the applied rf frequency. This assumption has been discussed by Bloembergen[19] and by Portis,[6] and appears to be justified in this case because of the possibility of mutual spin flips between neighboring nuclei brought about by the dipolar interaction. The third assumption of the BPP theory is that the complex rf susceptibility is proportional to the difference in population of the nuclear spin levels and is not affected by the presence of the rf field except in so far as the spin level populations are. When the spin system becomes saturated the populations of the spin levels become more nearly equal and it follows directly from this assumption that both the real and imaginary parts of the rf susceptibility saturate in the same way.

If the line shape is assumed to be Lorentzian[20] below saturation, the predictions of the BPP theory are in agreement with those of the Bloch equations (under steady-state conditions) and, apparently, with experiment in the case of most gases and liquids. As discussed below, the BPP theory also predicts the correct asymptotes for χ'' in solids for the limits $H_1 \to 0$ and $H_1 \to \infty$, and, therefore, the correct qualitative behavior of χ'' over the whole range of H_1 (except in the special case of inhomogeneity broadening).[6] The BPP prediction of the variation of M_z just at the onset of saturation is also correct. Evidently, these predictions are valid in solids because they are based only on the first two assumptions of the BPP theory. The predictions concerning the dispersion above saturation, which are in marked disagreement with the experimental data of Sec. II, are a consequence of the third assumption, and it appears certain that the trouble lies here.

Bloembergen[19] has pointed out that the BPP theory must be incorrect when a large rf field is applied to a solid in which $T_1 \neq T_2$ because in the limit as $H_1 \to \infty$ the line width is predicted to be $\gamma H_1 \sqrt{(T_1/T_2)}$ rather than γH_1 as expected from the uncertainty principle and the transition probability associated with the rf field.

The assumption that the complex susceptibility is proportional to the difference in population of the adjacent nuclear spin levels is equivalent to the assumption that the spin system behaves as if it were at equilibrium at a spin temperature higher than the lattice temperature, corresponding to the actual distribution of
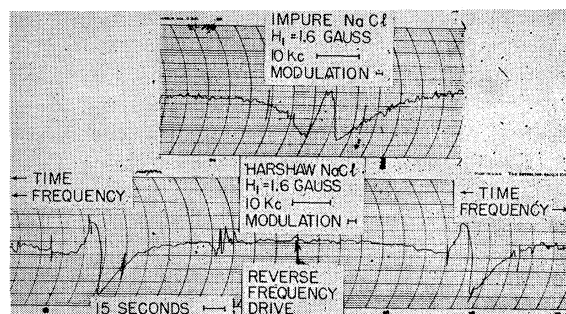

FIG. 5. Apparent dispersion derivatives in samples of NaCl of different purity. The Na[23] nucleus was observed at a frequency of about 7.5 megacycles. The modulation frequency was 41 cps in phase with the lock-in detector.

nuclear spins among the $2I+1$ levels. Evidently, the assumption of an equilibrium distribution of spin states, i.e., a spin temperature, is not justified in the case of saturation, where the spins are subject to a large time-dependent secular perturbation. Although the amplitudes of the spin states may be described by a Boltzmann distribution, the phases of the quantum states are not random, as would be the case[21] at thermal equilibrium and as is required in most quantum-mechanical perturbation calculations. This can be seen from the fact that M_x and M_y, the transverse components of nuclear magnetization, are not zero and cannot in general be made arbitrarily small compared with M_z if the system is saturated. A random distribution of quantum phases would lead to zero transverse magnetization. For this reason it is surprising that the simple assumption of a spin temperature predicts the same behavior for a Lorentzian line as the more detailed assumptions of the Bloch equations.

The Bloch equations[4] are based on the assumptions that the interaction of the spins with the lattice and with each other can be considered independently of their interaction with the externally applied magnetic field, and that the effect of spin-lattice and spin-spin interactions can be described by simple relaxation terms. They predict a Lorentzian line shape and saturation behavior similar to that predicted by BPP, apparently in good agreement with experiment for most liquids and gases. Detailed theoretical justification of the Bloch equations has been given by Wangsness and Bloch[22] and by Kubo and Tomita,[23] but their work is applicable only to liquids and gases in which the correlation time of the motion of the nuclei is short compared to the Larmor period. These authors neglect the effect of the rf field on the relaxation process, and Bloch and Wangsness also consider the spins as independent of each other, which, as they recognize, is not justified in the case of solids.

[19] N. Bloembergen, thesis, Leiden (unpublished), p. 49.
[20] G. E. Pake and E. M. Purcell, Phys. Rev. 74, 1184 (1948); 75, 534 (1949).
[21] R. C. Tolman, Principles of Statistical Mechanics (Oxford University Press, New York, 1930), Chap. IX.
[22] R. K. Wangsness and F. Bloch, Phys. Rev. 89, 728 (1953).
[23] R. Kubo and K. Tomita, J. Phys. Soc. (Japan) 9, 888 (1954).

The Bloch equations have always been recognized as a crude approximation for solids well below the melting point, since they predict a Lorentzian line shape rather than the nearly Gaussian shape[20] observed experimentally. Thus it is natural to suppose that the spin-spin terms of the Bloch equations (those involving T_2) are the source of the present difficulty. This can be seen in more detail by considering a specific solution of these equations.

Suppose that a circularly polarized rf field of magnitude H_1 and frequency ω_0 (the resonance frequency) is continuously applied to the solid, and suppose that initially the nuclear magnetization $\mathbf{M}$ is in the direction of the rf field and of magnitude M_1. Assume that $T_1 \gg T_2$ as is the case in most solids at low temperatures. The terms in the Bloch equations involving T_1 can then be neglected during a time comparable to T_2, and the prediction of the Bloch equations is that $\mathbf{M}$ will remain parallel to $\mathbf{H}_1$ and will decay exponentially to zero in a time T_2.

In the course of this decay work $M_1 H_1$ is done by the spin system on the external magnetic field; this energy can come only from the internal (spin-spin) energy of the spin system. The energy cannot come from the lattice, because we have implicitly neglected the spin-lattice interaction by neglecting the T_1 term in the Bloch equations. Speaking somewhat classically and loosely we can say that the initial state corresponds to n excess spins aligned in the rf field direction and the final state corresponds to no excess spins aligned in any specific direction and $\mathfrak{N}$ excess spins aligned preferentially in the direction of the magnetic fields of their neighbors. Conservation of energy requires that

$$nH_1 = \mathfrak{N}\delta H, \tag{6}$$

where δH is of the order of the rms magnetic field at a nucleus due to its neighbors, or approximately the half-width of the resonance line in gauss.

The decay predicted in time T_2 by the Bloch equations is an irreversible process in a thermally isolated spin system, and the entropy of the system must increase. The initial entropy of the spin system is the same as that for a spin system with n excess spins parallel to a fixed magnetic field:

$$S_i = S_0 - kn^2/N. \tag{7}$$

S_0 is the maximum entropy of the spin system corresponding to complete chaos, k is Boltzmann's constant, N is the total number of spins, and for simplicity we assume that the spin is $\frac{1}{2}$.

By analogy with (7), the entropy of the final state is expected to be approximately given by

$$S_F = S_0 - k\mathfrak{N}^2/N. \tag{8}$$

This assumption can be justified by a detailed calculation similar to that of Appendix A discussed below.

From (6), (7), and (8) it follows that the spin entropy increases during the decay only if $H_1 \lesssim \delta H$. Thus for sufficiently large H_1 the Bloch equations are evidently incorrect, because they predict an irreversible process in which the entropy decreases.

The actual final value of $\mathbf{M}$ after such a transverse decay can be estimated by maximizing the entropy, subject to the condition that energy must be conserved. We assume that the entropy is $S_0 - k(n^2 + \mathfrak{N}^2)/N$ and require that $nH_1 + \mathfrak{N}\delta H$ be a constant. If $\mathfrak{N}$ is initially zero the entropy is a maximum if n, and therefore M, is finally $[1 + (\delta H)^2/H_1^2]^{-1}$ times its initial value, and the external energy $-MH_1$ is $H_1^2/(\delta H)^2$ times the internal spin-spin energy.

To summarize, for $H_1 \gtrsim \delta H$ the spin system is unable to take up the entire energy of the nuclear magnetization with respect to the rf magnetic field, and the transverse decay predicted by the Bloch equations is partially forbidden. As will be discussed in the next section such a process is further inhibited by the rapid decrease of the suitable transition probabilities as the rf field is increased.

These considerations suggest that in the limit of large H_1 the x,y components of the Bloch equations should be modified. The modification can most easily be presented in a coordinate system[24] rotating about the z-axis at the rf frequency ω (not necessarily the resonance frequency) with its x-axis in the direction of the circularly polarized rf field H_1. In such a coordinate system the modified Bloch equations are

$$\dot{M}_{xr} = \gamma[\mathbf{M}_r \times \mathbf{H}_{er}]_{xr} - M_{xr}/T_{2e}, \tag{9a}$$

$$\dot{M}_{yr} = \gamma[\mathbf{M}_r \times \mathbf{H}_{er}]_{yr} - M_{yr}/T_2, \tag{9b}$$

$$\dot{M}_{zr} = \gamma[\mathbf{M}_r \times \mathbf{H}_{er}]_{zr} - (M_{zr} - M_0)/T_1. \tag{9c}$$

The subscript r denotes a quantity measured with respect to the rotating coordinate system, and H_{er} is the effective magnetic field.[23] $\mathbf{H}_{er}$ is given by

$$\mathbf{H}_{er} = \left(H_0 - \frac{\omega}{\gamma}\right)\mathbf{k}_r + H_1\mathbf{i}_r, \tag{10}$$

where $\mathbf{i}_r$ and $\mathbf{k}_r$ are unit vectors in the x_r and z_r directions in the rotating system.

In (9) T_{2e} is of the order of T_1 and is a transverse spin-lattice relaxation time, since, as discussed at length above, the spin-spin collisions are unable to relax the magnetization in the direction of a large rf field. T_2 is still the correct relaxation time to use in the y-component of (9) because a decay in the y-direction (rotating frame of reference) involves no change in energy. Solution of (9) leads to the prediction

$$\chi' = \frac{\frac{1}{2}\chi_0 T_2 T_{2e}\omega_0(\omega_0 - \omega)}{(\omega - \omega_0)^2 T_2 T_{2e} + \gamma^2 H_1^2 T_1 T_2 + 1} \tag{11a}$$

$$\chi'' = \chi' T_{2e}^{-1}(\omega_0 - \omega)^{-1}. \tag{11b}$$

[24] Rabi, Ramsey, and Schwinger, Revs. Modern Phys. **26**, 167 (1954), to which the reader is referred for an excellent introduction to the use of rotating coordinates.

The Lorentzian dispersion predicted by (11a) is in reasonable agreement with both the shape and order of magnitude of the observed dispersion at high rf fields. Unfortunately (11) is quantitatively applicable only at the highest rf fields attainable. To obtain quantitative results at lower rf fields it is necessary to consider the problem in more detail.

To conclude our discussion of the existing saturation theories we may mention another defect in the Bloch equations. As usually written,[4] they predict that the effect of the spin-lattice interaction is to relax the nuclear magnetization toward its static equilibrium value $\chi_0 H_0 \mathbf{k}$ in time T_1, where $\mathbf{k}$ is a unit vector in the z direction. Actually it is more reasonable to assume that the magnetization relaxes toward the value $\chi_0 \mathbf{H}$ corresponding to the instantaneous applied field $\mathbf{H}$. The theory and experiment in the present paper will be restricted to the case $H_0 \gg H_1$ so that $H_0 \mathbf{k}$ and $\mathbf{H}$ very nearly coincide in magnitude and direction, and this consideration is unimportant.

B. Rotating Coordinate Representation

If we neglect the interaction with the lattice, the complete Hamiltonian of the spin system is[25]

$$\mathcal{3C}_s = g\beta H_0 \sum_j I_{jz} + g\beta 2H_1(\cos\omega t)\sum_j I_{jx}$$
$$+ g^2\beta^2 \sum_{k>j}(r_{jk}^{-3}\mathbf{I}_j\cdot\mathbf{I}_k - 3r_{jk}^{-5}\mathbf{r}_{jk}\cdot\mathbf{I}_j\ \mathbf{r}_{jk}\cdot\mathbf{I}_k)$$
$$+ \sum_{k>j}\tilde{A}_{jk}\mathbf{I}_j\cdot\mathbf{I}_k, \quad (12)$$

where H_0 is the dc field, $2H_1$ is the applied linearly polarized rf field[12] of frequency ω, and the spin operators I_j are expressed in units of $\hbar$. All nuclei are assumed to have the same g-factor and spin; the case of two magnetic ingredients will be considered later. The last term is included for generality; evidence for the existence of such a mutual nuclear interaction in solids has been discussed by Bloembergen and Rowland[26] and by Ruderman and Kittel.[27] The analogous interaction between nuclei in molecules was first suggested by Ramsey and Purcell.[28]

The spin wave function ψ obeys Schrödinger's equation:

$$-i\hbar\dot{\psi} = \mathcal{3C}_s\psi. \quad (13)$$

We will use the transformations

$$\psi = R_{y\Theta}\psi_r = R_{y\Theta}R_{z\omega t}\psi_\rho, \quad (14)$$

where

$$R_{z\omega t} = \exp(-i\omega t\sum_j I_{jz}), \quad (15)$$

$$R_{y\Theta} = \exp(-i\Theta\sum_j I_{jy}), \quad (16)$$

$$\Theta = \tan^{-1}[\gamma H_1/(\omega-\omega_0)]. \quad (17)$$

[25] J. H. Van Vleck, Phys. Rev. 74, 1168 (1948).
[26] N. Bloembergen and T. J. Rowland, Phys. Rev. 97, 1679 (1955).
[27] M. A. Ruderman and C. C. Kittel, Phys. Rev. 96, 99 (1954).
[28] N. F. Ramsey and E. M. Purcell, Phys. Rev. 85, 143 (1952).

Then it follows that

$$-i\hbar\partial\psi_r/\partial t = (-\hbar\omega\sum_j I_{zj}$$
$$+ R_{z\omega t}\mathcal{3C}_s R_{z\omega t}^{-1})\psi_r \equiv \mathcal{3C}_{er}\psi_r, \quad (18)$$

and

$$-i\hbar\partial\psi_\rho/\partial t = R_{y\Theta}\mathcal{3C}_{er}R_{y\Theta}^{-1}\psi_\rho \equiv \mathcal{3C}_{e\rho}\psi_\rho. \quad (19)$$

The unitary transformation $R_{z\omega t}$ can be regarded as a transformation to a coordinate system rotating about the z-axis with frequency ω (note that this is the rf frequency, not necessarily the resonance frequency ω_0). As above, the subscript r is used to denote quantities in this coordinate system and $\mathcal{3C}_{er}$ is the effective Hamiltonian in the r-system.

$R_{y\Theta}$ corresponds to a further transformation to a coordinate system fixed with respect to the r-system, whose z-axis coincides with the effective magnetic field direction, and whose y-axis coincides with the y-axis of the r-system. Θ is the angle between the effective magnetic field $\mathbf{H}_{er}$ in the rotating coordinate system[24] and the z-axis in the fixed system. Quantities in this system are denoted by the subscript ρ.

The Hamiltonians $\mathcal{3C}_{er}$ and $\mathcal{3C}_{e\rho}$ in (18) and (19) are readily obtained from the fact that the operators $\mathbf{I}_j$ transform like vectors under the rotations corresponding to $R_{z\omega t}$ and $R_{y\Theta}$. Since the $\mathbf{I}_j$ occur only in scalar products the same result can be achieved by applying the inverse rotation to the other vector of the scalar product. Thus $\mathbf{I}_j\cdot\mathbf{I}_k$ is invariant under these transformations while the $\mathbf{r}_{jk}$ are transformed under the inverse rotation. This procedure is simply an algebraic shortcut; actually the $\mathbf{r}_{jk}$ are invariant parameters and the $\mathbf{I}_j$ undergo transformation. In this way we get

$$\mathcal{3C}_{er} = g\beta\mathbf{H}_{er}\cdot\sum_j \mathbf{I}_j + \sum_{k>j}(A_{jk}\mathbf{I}_j\cdot\mathbf{I}_k + B_{jk}I_{jz}I_{kz})$$
$$+ \text{time-dependent part}, \quad (20)$$

$$\mathcal{3C}_{e\rho} = g\beta H_{er}\sum_j I_{jz} + \sum_{k>j}\{A_{jk\rho}\mathbf{I}_j\cdot\mathbf{I}_k + B_{jk\rho}I_{jz}I_{kz}$$
$$+ D_{jk\rho}[I_{j+}I_{k+} + I_{j-}I_{k-}]$$
$$+ E_{jk\rho}[(I_{j+}+I_{j-})I_{kz} + I_{jz}(I_{k+}+I_{k-})]\}$$
$$+ \text{time-dependent part}, \quad (21)$$

where

$$A_{jk} = \tilde{A}_{jk} + g^2\beta^2 r_{jk}^{-3}(\tfrac{3}{2}\xi_{jk}^2 - \tfrac{1}{2}), \quad (22)$$

$$B_{jk} = -3g^2\beta^2 r_{jk}^{-3}(\tfrac{3}{2}\xi_{jk}^2 - \tfrac{1}{2}), \quad (23)$$

$$A_{jk\rho} = \tilde{A}_{jk} + (\tfrac{3}{2}\cos^2\Theta - \tfrac{1}{2})(A_{jk} - \tilde{A}_{jk}), \quad (24)$$

$$B_{jk\rho} = (\tfrac{3}{2}\cos^2\Theta - \tfrac{1}{2})B_{jk}, \quad (25)$$

$$D_{jk\rho} = \tfrac{1}{4}\sin^2\Theta B_{jk}, \quad (26)$$

$$E_{jk\rho} = \tfrac{1}{2}\sin\Theta\cos\Theta B_{jk}, \quad (27)$$

$$H_{er} = |\mathbf{H}_{er}| = [H_1^2 + (H_0 - \omega/\gamma)^2]^{\frac{1}{2}}. \quad (28)$$

Here $I_{j\pm}$ are the raising and lowering operators $I_{jx}\pm iI_{jy}$ having selection rules $\Delta M_{Ij} = \pm1$ respectively, and ξ_{jk} is the z-direction cosine of $\mathbf{r}_{jk}$. The time dependent parts of these Hamiltonians contain terms like $I_{j\pm}I_{k\mp}$, $I_{j\pm}I_{kz}$, $I_{j\pm}I_{k\pm}$, etc., with time dependences $\exp(\pm i\omega t)$, $\exp(\pm 2i\omega t)$.

We now assume $H_0 \gg H_{er} \cong \delta H$ and apply Dirac perturbation theory to Schrödinger's equation in the rotating coordinate systems [Eqs. (18) and (19)]. The time-dependent part of $\mathfrak{IC}_{er}$ (or $\mathfrak{IC}_{ep}$) is a nonsecular perturbation on the time-independent part. It connects states for which $\Delta M_I = \pm 1$ for one or two nuclei, and for it to be secular these states must differ in effective energy[29] by $\pm \hbar \omega \cong \pm \gamma \hbar H_0$ or $\pm 2\hbar \omega \cong 2\gamma \hbar H_0$. Actually such states will differ in effective energy[29] by about $c\gamma \hbar (H_{er} \pm \delta H)$, with $c = 0$, 1, or 2, so the condition for a secular perturbation is not satisfied and the time-dependent part of $\mathfrak{IC}_{er}$ can be ignored for most purposes.[30] It will be noted that these time-dependent terms are the same ones neglected by Van Vleck[25] in his calculation of the moments of the absorption line, plus a term corresponding to the component of applied rf field rotating in the opposite direction from that of the rotating coordinate system.

If H_{er} is very large (but still much less than H_0) the fourth and fifth terms of $\mathfrak{IC}_{ep}$ are nonsecular perturbations, since, being time-independent, to be secular they must connect eigenstates of the first three terms of $\mathfrak{IC}_{ep}$ having the same effective energy, whereas actually they connect states differing in effective energy by about one or two times $\gamma \hbar (H_{er} \pm \delta H)$. Under these circumstances we can ignore these terms and $\mathfrak{IC}_{ep}$ conserves M_{zp}, the nuclear magnetization in the effective field direction. It should be noted that to ignore these terms the transition probabilities associated with them must be much smaller than T_1^{-1}. Thus this procedure is valid only for H_{er} very much larger than the resonance line width.

Conservation of M_{zp} leads to a system of equations similar to (9), whose solution in the limit of large H_1 is identical with (11). We do not go into details because the theory is not applicable to any experimentally attainable situation. Experimentally we are limited to rf field intensities comparable to the resonance line width.

C. Canonical Distribution in the Rotating System

In the previous section we obtained a transformed spin Hamiltonian which was effectively independent of time. A time-independent Hamiltonian is convenient to work with because the concepts of statistical mechanics can be more easily applied to it and because the effective energy[29] of the spin system can change only through the

[29] "Effective energy" will be used to denote effective energy with respect to the rotating coordinate system, i.e., with respect to the time independent part of $\mathfrak{IC}_{er}$ or $\mathfrak{IC}_{ep}$, not the total energy in the fixed system, which is no longer a constant of the motion. The word "effective" will denote any quantity defined or measured in the rotating system.

[30] If $H_{er} < \delta H$ it becomes questionable to ignore the time-dependent part of $\mathfrak{IC}_{er}$, since then this "perturbation" is larger than the "unperturbed" part of the Hamiltonian. For the same reason it may be incorrect to ignore the oppositely rotating component of circularly polarized rf field which is always present when a linearly polarized field is applied. These considerations are probably not as important as might be thought, because these perturbations are very far from secular; furthermore, experimental evidence discussed below indicates that transitions produced by these time dependent parts of $\mathfrak{IC}_{er}$ and $\mathfrak{IC}_{ep}$ are negligible.

spin-lattice interaction. The spin-lattice interaction terms of the Hamiltonian acquire an additional explicit time dependence as a result of the transformation to the rotating system, but if H_{er} is large enough, these terms can be considered as a small perturbation which transfers effective energy between the spin system and the lattice and eventually determines the value of the effective energy of the spin system.

As in the statistical mechanics of stationary systems we consider a Gibbsian ensemble of systems, each consisting of the solid with the rf field continously applied to it. Suppose that the (time-dependent) spin-lattice interaction is somehow turned off, and that the average expectation values of the lattice Hamiltonian and transformed spin Hamiltonian $(\mathfrak{IC}_{er})$ are known. In the absence of further information the distribution of states in the ensemble is still highly ambiguous, but the *most probable* distribution is a canonical distribution of states with respect to the lattice and the *transformed* Hamiltonian. Associated with this canonical distribution are two temperatures, determined by the canonical average expectation values of the lattice and transformed spin Hamiltonians. One of these is the lattice temperature, which is presumably positive in any physically attainable solid. The other will be called the effective spin temperature, which is positive or negative depending on whether the average expectation value of the effective spin Hamiltonian $\mathfrak{IC}_{er}$ is negative or positive. The situation is closely analogous to that in the fixed coordinate system if the spin-lattice interaction is turned off and if no rf field is applied. In that case the most probable state of the system is also represented by a canonical distribution of states, with lattice and spin temperatures which are not necessarily equal. Negative spin temperatures are easily attained (with pulse techniques) in insulating crystals in which the spin-lattice interaction is very small. In both the fixed and the rotating coordinate systems the lattice and (effective) spin temperatures can be different because the spin and lattice Hamiltonians commute, and it is sensible to talk about canonical distributions of states only because the lattice and (effective) spin Hamiltonians are time-independent (except for some nonsecular perturbations) in both cases.

We now consider what happens if we turn on the spin-lattice interaction and wait for a time long compared to the spin-lattice relaxation time, but short compared to the time required for the rf field to heat up the lattice appreciably. In the absence of the rf field and in the fixed coordinate system, the spin system will approach a canonical distribution of states with equal spin and lattice temperatures. In the presence of the rf field, in the rotating system, the spin-lattice interaction will change the average expectation value of the effective spin Hamiltonian to some quasi-equilibrium value. We have no rigorous assurance that the spin system will remain in a canonical distribution of states with respect to $\mathfrak{IC}_{er}$ but we *assume* that it will. This assumption can

be regarded as an admission of our ignorance concerning the system; lacking detailed information, we simply assume that the system is in its most probable state for the limit of zero spin-lattice interaction. The actual effective spin temperature in the steady state is determined by the lattice temperature and the spin-lattice interaction, and depends on H_0, H_1, and ω. Unlike the static case with no rf field, the effective spin temperature is different from the lattice temperature and can actually be negative. The reason for this difference is that the spin-lattice interaction in the rotating system contains an explicit time dependence which is not present in the fixed system.

An analogous problem is that of a gas in a fairly well-insulated bottle, connected to one or more temperature baths by heat leaks. To find, say, the pressure of the gas it is necessary to assume immediately that the gas molecules are in their most probable state (a Boltzmann distribution) subject to the constraint that they have some definite energy (corresponding to the gas temperature). The problem is then reduced to finding the gas temperature as determined by the various heat leaks (corresponding to the spin-lattice interaction) and temperature baths (corresponding to the lattice). If the bottle is constrained to move it is necessary to transform to the bottle's coordinate system before applying statistical mechanics to the gas, in analogy to the rotating coordinate transformation used here. All of classical acoustics and fluid mechanics are based on assumptions similar to those used in this paper since it is always assumed that matter possesses the same thermodynamic properties viewed from a suitably moving coordinated system and in suitably small pieces as it does at rest in a fixed coordinate system. When temperature, pressure, or velocity gradients in a gas become too large, this assumption breaks down (i.e., at low pressures and in shock waves) and the theory becomes difficult. Likewise, in the case of spins when the spin-lattice interaction becomes too large, the assumptions used here break down and the theory is difficult.

A rigorous justification of this procedure would be extremely difficult, if not impossible. It might be based on something analogous to the Boltzmann H-theorem. The least that can be said for this assumption is that above saturation it is the only simple one that is not obviously wrong.

The assumption that the spin system is in a canonical distribution of states with respect to $\mathfrak{IC}_{er}$ leads immediately to the conclusion that the magnetization $\mathbf{M}_r$ is in the direction of the effective field $\mathbf{H}_{er}$, just as in the static case the magnetization $\mathbf{M}$ is in the direction of $\mathbf{H}_0$. The effective external energy of the spin system is $-\mathbf{M}_r \cdot \mathbf{H}_{er} = -M_{z\rho}H_{er}$, where $M_{z\rho}$ is the z_ρ component of magnetization in the ρ coordinate system. We define a spin-spin energy in the rotating system which contains all the spin-spin terms of $\mathfrak{IC}_{er}$:

$$\mathfrak{IC}_{SS} = \sum_{j>k}(A_{jk}\mathbf{I}_j \cdot \mathbf{I}_k + B_{jk}I_{jz}I_{kz}). \qquad (29)$$

The internal spin-spin energy is comparable to the external energy when the effective external field H_{er} becomes comparable to the local fields at the nuclei due to their neighbors (i.e., approximately the line width in gauss) just as in the static case.[31] In Appendix A it is shown that

$$\langle\langle\mathfrak{IC}_{SS}\rangle\rangle = -[(\delta H)^2/H_{er}^2]M_{z\rho}H_{er}, \qquad (30)$$

where $\langle\langle O\rangle\rangle$ denotes the canonical average expectation value of the operator O, and

$$(\delta H)^2 = \tfrac{1}{3}\langle(\Delta H)^2\rangle_{\mathrm{Av}} + \frac{I(I+1)}{\hbar^2\gamma^2 N}\sum_{k>i}\tilde{A}_{jk}^2. \qquad (31)$$

Here $\langle(\Delta H)^2\rangle_{\mathrm{Av}}$ is the second moment of the unsaturated resonance line as calculated by Van Vleck.[25]

The reasoning which leads to (30) is essentially the same as that used in Sec. III(b) to find the state of maximum entropy of the spin system after a transverse Bloch decay, and the $(\delta H)^2$ used there is the quantity given by (31). The state of maximum entropy of a system for a given energy is, of course, described by the canonical distribution of states corresponding to that energy.

The problem is solved if the value of $\langle\langle\mathfrak{IC}_{er}\rangle\rangle$ can be determined, because we can write

$$\begin{aligned}\langle\langle\mathfrak{IC}_{er}\rangle\rangle &= -M_{z\rho}H_{er} + \langle\langle\mathfrak{IC}_{SS}\rangle\rangle \\ &= -M_{z\rho}H_{er}[1+(\delta H)^2/H_{er}^2].\end{aligned} \qquad (32)$$

Transforming back to the fixed system we have (since $\mathbf{M}_r$ is in the direction of $\mathbf{H}_{er}$)

$$M_x \simeq M_{z\rho}\sin\Theta\cos\omega t, \qquad (33a)$$

$$M_y \simeq M_{z\rho}\sin\Theta\sin\omega t, \qquad (33b)$$

$$M_z \simeq M_{z\rho}\cos\Theta. \qquad (33c)$$

To determine the expectation value of $\mathfrak{IC}_{er}$ we use a simple relaxation assumption to account for the spin-lattice interaction. The physical reasoning which follows is justified in more detail and under more general conditions in Appendix B. We assume here that the effect of the spin-lattice interaction is to relax each nucleus independently into its equilibrium state in a time T_1:

$$[\partial/\partial t]_{SL}\langle\langle\mathbf{I}_j\rangle\rangle = -(\langle\langle\mathbf{I}_j\rangle\rangle - \mathbf{I}_0)/T_1, \qquad (34)$$

where the left-hand side is the spin-lattice contribution to the time derivative of the expectation value of $\mathbf{I}_j$, and $\mathbf{I}_0$ is the static thermal equilibrium value of $\mathbf{I}_j$, given by

$$\mathbf{I}_0 = \tfrac{1}{3}g\beta I(I+1)\mathbf{H}/kT. \qquad (35)$$

Here the applied field $\mathbf{H}$ can be closely approximated by $H_0\mathbf{k}$ (since $H_1 \ll H_0$).

It might seem more logical to assume that the nuclei are relaxed along the effective field instead of the actual applied field, so that we should use $\mathbf{H}_{er}$ in (35) instead of $\mathbf{H}$. That this would be incorrect follows from the fact

[31] J. H. Van Vleck, J. Chem. Phys. 5, 320 (1937).

that the electrons, which are responsible for the relaxation, are almost completely unaffected by the rf field and effectively see only the large field H_0 in the z-direction. Furthermore, if we were to use the effective field in (35) we would get obviously incorrect predictions for the dispersion.

Equation (34) implies that T_{2e}, the transverse electronic relaxation time defined previously, is equal to T_1. This assumption is in accord with theory[12,23,32] for metals, assuming the electrons are in a Fermi distribution of states.

We assume that the spin-lattice interaction does not perturb the spin system cononical distribution appreciably except to bring about a slow change in $\langle\langle \mathcal{3C}_{er} \rangle\rangle$ $=\langle\langle \mathcal{3C}_{e\rho} \rangle\rangle$, the transformed spin Hamiltonian average expectation value. The spin lattice relaxation can be fictionally regarded as a two-step process. The first process is the scattering of the nuclear spin into a completely random orientation, in a time T_1. The second process is a scattering of the spin into an orientation with probability governed by the Boltzmann distribution of states with respect to the externally applied magnetic field, in an infinitesimal time after the first scattering. These two processes correspond respectively to the two terms on the right-hand side of (34). The change in $\langle\langle \mathcal{3C}_{er} \rangle\rangle$ with time is the sum of the separate changes brought about by these two processes.

The rate of change of $\langle\langle \mathcal{3C}_{er} \rangle\rangle$ due to the first (random) scattering is

$$[\partial/\partial t]_{SLR}\langle\langle \mathcal{3C}_{er} \rangle\rangle = +M_{z\rho}H_{er}/T_1 - 2\langle\langle \mathcal{3C}_{SS} \rangle\rangle/T_1. \quad (36)$$

The external effective spin energy $-M_{z\rho}H_{er}$ (expectation value of the first term of $\mathcal{3C}_{er}$) is proportional to the sum of expectation values of components of the $\mathbf{I}_j$, and is thus expected to decay to zero in time T_1 for random scattering of the spins, corresponding to the first term in (36). The spin-spin energy $\langle\langle \mathcal{3C}_{SS} \rangle\rangle$, on the other hand, is quadratic in the components of the $\mathbf{I}_j$, and is therefore expected to decay at twice the relative (logarithmic) rate of the external energy; thus the factor two in the last term of (36).

The effect of the second (Boltzmann) scattering is to change the nuclear magnetization at a rate $+\mathbf{M}_0/T_1$, where $\mathbf{M}_0 = \chi_0\mathbf{H} \simeq \chi_0 H_0\mathbf{k}$ (in the fixed coordinate system). The corresponding rate of increase of the effective external energy $-\mathbf{M}\cdot\mathbf{H}_{er}$ is $-(\mathbf{M}_0/T_1)\cdot\mathbf{H}_{er}$. The change in the spin-spin energy is negligible, since the local fields at the nuclei are random in orientation, to a very good approximation. Thus the rate of change of $\langle\langle \mathcal{3C}_{er} \rangle\rangle$ due to the Boltzmann scattering is the same as that of the effective external energy:

$$[\partial/\partial t]_{SLB}\langle\langle \mathcal{3C}_{er} \rangle\rangle = -M_0 H_{er}\cos\Theta/T_1. \quad (37)$$

To obtain the steady-state value of $M_{z\rho}$ we use (30) and (32), and set the sum of (36) and (37) equal to zero.

---

[32] N. Bloembergen (private communication).

The result is

$$M_{0\rho} = \frac{M_0\cos\Theta}{1+2(\delta H)^2/H_{er}^2}, \quad (38)$$

where $M_{0\rho}$ is the quasi-equilibrium value of $M_{z\rho}$ for constant H_0, H_1, and ω.

The dispersion is given by

$$\chi' = \frac{M_{xr}}{2H_1} = \frac{M_{0\rho}\sin\Theta}{2H_1}, \quad (39)$$

or

$$\chi' = \frac{M_0\gamma(\omega_0-\omega)}{2\{(\omega_0-\omega)^2+\gamma^2[H_1^2+2(\delta H)^2]\}}, \quad (40)$$

so that above saturation the dispersion is Lorentzian and the dispersion derivative at resonance is

$$\frac{\partial\chi'}{\partial H_0} = \frac{\chi_0 H_0}{2[H_1^2+2(\delta H)^2]}. \quad (41)$$

Equation (33) implies that the nuclear magnetic absorption is zero above saturation. Actually, (33) is an approximation and $\mathbf{M}_r$ is not precisely in the direction of $\mathbf{H}_{er}$. At any rf level there is finite absorption which can be predicted by invoking conservation of energy in the fixed system. Energy is transferred from the spin system to the lattice at a rate $-H_0(M_z-M_0)/T_1$. Equating this to the energy absorbed by the spin system from the rf field, which is $2\omega H_1^2\chi''$, we get

$$\chi'' \cong H_0(2H_1\chi'\cot\Theta - M_0)/2T_1 H_1^2\omega, \quad (42)$$

or

$$\chi'' = \frac{\gamma^2[H_1^2+2(\delta H)^2]H_0 M_0}{2\{(\omega-\omega_0)^2+\gamma^2[H_1^2+2(\delta H)^2]\}T_1 H_1^2\omega}. \quad (43)$$

This is a Lorentzian line, of the same width as would be predicted by the Bloch equations below saturation for $T_2 = \gamma^2[H_1^2+2(\delta H)^2]^{-1}$. At resonance (43) agrees with the asymptotic values of χ'' given by the Bloch and BPP theories. The same is true of off resonance in the limit of very large H_1. This agreement corresponds to the fact that, for any theory, under these conditions $M_z \rightarrow 0$ and χ'' is uniquely determined by this simple conservation of energy argument. The fact that all theories yield the same asymptotic χ'' means that the saturation method of obtaining T_1 used in Sec. II is substantially correct. This is not necessarily true if the maximum absorption derivative, rather than the integrated absorption derivative, is used to obtain T_1. Error in the saturation determination of T_1 can also be introduced by the use of a magnetic field modulation period comparable with or less than T_1, as is usually the case experimentally. Fast modulation is treated in Sec. III(e).

The theory developed above is valid only for large H_{er}. If H_{er} becomes comparable to the value of H_1 at which the absorption begins to saturate, the spin-lattice

interaction can no longer be regarded as a small perturbation and the magnetization $\mathbf{M}$ will tend toward the z-axis with a value M_0, rather than toward the direction of H_{er}. Treatment of the intermediate case would be extremely difficult.

The theory is also invalid in the case of large H_{er} but small H_1; i.e., in the case of $\Theta \simeq 0$ or $\Theta \simeq \pi$ (off resonance). In this case the spin-lattice interaction is still in a sense a small perturbation, but the last two terms of $\mathcal{K}_{ep}$ approach zero. These terms help bring about the transfer between external and internal effective spin energy which is required by the assumption of a canonical distribution of spin states with respect to $\mathcal{K}_{ep}$. If the transition probabilities due to these terms are smaller than T_1^{-1}, then M_{zp} is conserved and the treatment at the end of the previous section applies. The fact that M_{zp} is conserved in the limit of small H_1 and finite H_{er} means that $M_{zp} \simeq M_z \simeq M_0$ in this case; i.e., the nuclear magnetization approaches its thermal equilibrium value, as is expected on elementary grounds.

We may summarize these limitations with the statement that the theory is valid in the range of H_1 well above the level where the absorption begins to saturate.

Some of the predictions of the theory are summarized in Fig. 6, which shows χ'' and $\partial \chi'/\partial H_0$ at resonance as a function of H_1. At low fields χ'' is determined by the line shape and the Kronig-Kramers relation for zero frequency:

$$\chi_0 = \frac{2}{\pi} \int_0^\infty \frac{\chi''(\nu)d\nu}{\nu}, \tag{44}$$

so that

$$\chi''(\nu_0) = \tfrac{1}{2}\pi\nu_0\chi_0 g(\nu_0). \tag{45}$$

The low rf field dispersion derivative, $\partial \chi'/\partial H_0$, is also determined by the Kronig-Kramers relations[20] and the line shape. We assume that the line is Gaussian. Using Eq. (11) of reference 20 (with the factor $\tfrac{1}{2}$ mentioned in the erratum)[20] and comparing Eq. (10), reference 20, with Eq. (15), reference 25, we get for a Gaussian line of second moment $\langle(\Delta H)^2\rangle_{\mathrm{Av}}$:

$$\partial \chi'/\partial H_0 = \chi_0 H_0/2\langle(\Delta H)^2\rangle_{\mathrm{Av}}. \tag{46}$$

This is the low rf field limit assumed in Fig. 6 for the case (curve a) of pure dipolar broadening ($\tilde{A}_{jk} = 0$). If there exists an exchange-type interaction ($\tilde{A}_{jk} \neq 0$) the resonance line will be exchange-narrowed and the dispersion derivative will be increased (curve b).

The region indicated by the dotted lines in Fig. 6 cannot be treated theoretically, but χ'' and $\partial \chi'/\partial H_0$ in this region are expected to undergo a smooth transition between their low and high rf field values, as indicated.

The solid lines in Fig. 6 for large H_1 represent the predictions of (41) and (43). In the limit of large H_1 the dispersion derivative is $M_0/2H_1^2$ (assuming $T_1 = T_{2e}$) independent of the spin-spin interaction. At intermediate values of H_1, for pure dipolar interaction
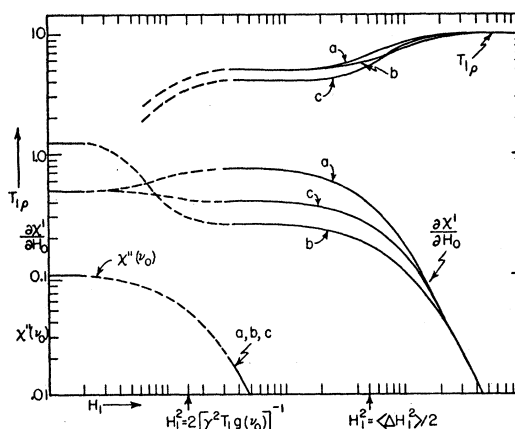

FIG. 6. Qualitative theoretical predictions of χ'', $\partial \chi'/\partial H_0$, and $T_{1\rho}$ at resonance for the cases of pure dipolar coupling (curve a), strong exchange-type coupling (curve b), and two magnetic ingredients (curve c). χ'' is in units of $5\pi\chi_0\nu_0 g(\nu_0)$, $\partial \chi'/\partial H_0$ is in units of $\chi_0 H_0/\langle(\Delta H)^2\rangle_{\mathrm{Av}}$, and $T_{1\rho}$ is in units of $T_1/10$.

($\tilde{A}_{jk} = 0$), (31), and (41) predict that $\partial \chi'/\partial H_0$ should approach a plateau of value $3\chi_0 H_0/4\langle(\Delta H)^2\rangle_{\mathrm{Av}}$ (curve a). The presence of exchange-type interaction will increase δH^2 and thus lower the height of the plateau (curve b).

In the theory outlined above it is implicitly assumed that parts of the spin-lattice interaction can be included in the spin Hamiltonian as classical perturbations. These parts are the Knight shift in metals and the chemical shift in insulators, accounted for by replacing H_0 by $H_0 + \Delta H$, and the possible mutual nuclear spin interactions due to the electrons in the solid, of which the last term of (12) is an example. We know of no rigorous justification for this splitting up of the spin-lattice interaction into stationary and relaxation parts, but it seems physically quite reasonable.

In insulating crystals, where spin diffusion[33] usually plays an important role in the relaxation process, the theory above may not be directly applicable, although the qualitative conclusions are apparently correct. Spin diffusion is expected to be affected by the presence of the large rf field. More specifically, (34) probably represents an oversimplification of the relaxation process.

In metals, (34) may also be an oversimplification of the actual relaxation process. Equation (34) would almost certainly hold if it were also time-averaged in a suitable way, but it probably does not represent the details of the nuclear relaxation correctly. In particular, the relaxation of neighboring nuclear spins by the conduction electrons may not be independent, but may instead be correlated in some way, owing to the finite extent of the electron wave functions. In this case the reasoning behind (37) would probably still be correct, but (36) would have to be replaced by the less specific equation

$$[\partial/\partial t]_{SLR}\langle\mathcal{K}_{er}\rangle = -\langle\mathcal{K}_{er}\rangle/T_{1\rho}, \tag{47}$$

[33] N. Bloembergen, Physica 15, 426 (1949).

where $T_{1\rho}$ is greater than $\frac{1}{2}T_1$ (for $T_{2e}=T_1$) for small H_1 and approaches T_1 (or in general T_{2e}) for large H_1. Equations (30), (32), (37), and (47) yield

$$M_{0\rho}=\frac{T_{1\rho}M_0\cos\Theta}{T_1[1+(\delta H)^2/H_{er}{}^2]},\qquad (48)$$

and at resonance

$$\frac{\partial\chi'}{\partial H_0}=\frac{T_{1\rho}\chi_0H_0}{2T_1[H_1{}^2+(\delta H)^2]}.\qquad (49)$$

$T_{1\rho}$ can be experimentally determined by observing the phase of the dispersion signal relative to the magnetic field modulation, as discussed in Sec. III(e) below.

Equation (47) may appear at first sight to be inconsistent with (36), when the spin relaxation is incoherent. Actually, this is not the case, since $\langle\langle\mathfrak{K}_{SS}\rangle\rangle$ and $M_{z\rho}H_{er}$ are related to $\langle\langle\mathfrak{K}_{er}\rangle\rangle$ by (30) and (32). If we solve these four equations for $T_{1\rho}$ we get the same expression obtained in Sec. III(e) in connection with the theory of fast modulation with incoherent relaxation [Eq. (63)].

Bloembergen[32] has suggested a method of calculating $T_{1\rho}$ in those metals for which the nuclear spin-spin interaction $A_{jk}\mathbf{I}_j\cdot\mathbf{I}_k$ is the predominant term in $\mathfrak{K}_{SS}$. This is the case[26,27] in most of the heavier metals, probably including copper and aluminum. Equation (47) can be written (assuming $T_1=T_{2e}$)

$$[\partial/\partial t]_{SLR}\langle\langle\mathfrak{K}_{er}\rangle\rangle=M_{z\rho}H_{er}/T_1-\langle\mathfrak{K}_{SS}\rangle/T_{SS}.\qquad (50)$$

The term $M_{z\rho}H_{er}/T_1$ in (50) is deduced in the same way as in (36). $T_{SS}{}^{-1}$ is a suitable average of the probability that, of two neighboring nuclei, either one will be flipped by an electron without the other. If the electron wavelength is very short it is expected that the relaxation will be incoherent and that $T_{ss}=\frac{1}{2}T_1$ as in (36).

T_{ss} can be estimated by considering nearest neighbors separated by a distance $\mathbf{r}_{jk}$. The important nuclear-electronic interaction is $A[(\mathbf{I}_j\delta(\mathbf{r}-\mathbf{r}_j)+\mathbf{I}_k\delta(\mathbf{r}-\mathbf{r}_k)]\cdot\mathbf{S}$, where $\mathbf{S}$ is the electronic spin operator and A is an interaction constant. For a transition involving $\mathbf{k}$ and $\mathbf{k}'=\mathbf{k}+\Delta\mathbf{k}$ as initial and final electronic propagation vectors this interaction becomes

$$\begin{aligned}
AP_F&(e^{i\Delta\mathbf{k}\cdot\mathbf{r}_j}\mathbf{I}_j+e^{i\Delta\mathbf{k}\cdot\mathbf{r}_k}\mathbf{I}_k)\cdot\mathbf{S}\\
&=\tfrac{1}{2}e^{-\Delta\mathbf{k}\cdot\mathbf{r}_k}AP_F\{(\mathbf{I}_j+\mathbf{I}_k)[\cos(\Delta\mathbf{k}\cdot\mathbf{r}_{jk})\\
&\quad+i\sin(\Delta\mathbf{k}\cdot\mathbf{r}_{jk})+1]\\
&\quad+(\mathbf{I}_j-\mathbf{I}_k)[\cos(\Delta\mathbf{k}\cdot\mathbf{r}_{jk})+i\sin(\Delta\mathbf{k}\cdot\mathbf{r}_{jk})-1]\}.\qquad (51)
\end{aligned}$$

$\mathbf{I}_j+\mathbf{I}_k$ commutes with $A_{jk}\mathbf{I}_j\cdot\mathbf{I}_k$ and thus does not contribute much to the decay of $\langle\langle\mathfrak{K}_{SS}\rangle\rangle$ unless the term $B_{jk}I_{jz}I_{kz}$ is relatively large. Assuming B_{jk} small, most of the relaxation of $\mathfrak{K}_{SS}$ results from the term involving $\mathbf{I}_j-\mathbf{I}_k$, with transition probabilities proportional to $2-2\cos(\Delta\mathbf{k}\cdot\mathbf{r}_{jk})$. We assume that the energy contours in k-space are spherical, in which case $k\simeq k'\simeq k_m$, the Fermi level value of k, and that all directions in

k-space are equally probable for the initial and final states. T_{SS} is then proportional to the average of $2-2\cos[(\mathbf{k}-\mathbf{k}')\cdot\mathbf{r}_{jk}]$ over all directions of k and k', keeping $k=k'=k_m$, and is normalized by the requirement $T_{SS}\to\frac{1}{2}T_1$ as $k_m\to\infty$. In this way we get

$$T_{SS}{}^{-1}\simeq2T_1{}^{-1}\{1-[1-\cos(2k_mr_{ij})]/2k_m{}^2r_{ij}{}^2\}.\qquad (52)$$

If it is assumed that there is one electron per atom in the Fermi gas, then $k_mr_{jk}=3.36$ for a face-centered cubic crystal and (52) indicates that $T_{SS}\simeq\frac{1}{2}T_1$, yielding almost the same predictions as (41) and (43). Only if $k_mr_{jk}\lesssim\pi/2$, or if the conduction band is almost filled and can be described as an almost empty band of positive holes with $k_mr_{jk}\lesssim\pi/2$, will there be an appreciable effect due to coherent relaxation of neighboring nuclei.

D. Two Magnetic Ingredients

There are two limiting cases to be considered when there are two or more types of spin in the lattice.

The first of these is typified by F-centers whose electron spin resonance is broadened by hyperfine interaction with the surrounding nuclear spins. Although the different F-centers in an alkali halide are magnetically coupled in theory via nuclear spin diffusion and direct interaction with each other, in fact such coupling is negligible over a length of time comparable to T_1 (electronic) because the spin-spin transitions involved are highly forbidden energetically by the relatively large local field differences experienced by the different spins. Then the F-centers must be regarded as decoupled and the assumption of a canonical distribution of states with respect to the transformed Hamiltonian abandoned. Portis[7] has developed an exact theory for this case.

The other limiting case is typified by two different nuclear species in the same crystal. In this case the local field differences between nuclei are relatively small and spin diffusion can take place.[33] Following Van Vleck we use primes to denote the spins whose resonance is not being observed; the rf frequency ω is supposed to be near the resonant frequency of the unprimed spins. The spin Hamiltonian is given by Van Vleck.[25] We transform to a rotating system as before, using the transformation $R_{z\omega t}$ in which the sum over the I_{jz} is carried out over all the nuclei, primed and unprimed. The transformed Hamiltonian is

$$\begin{aligned}
\mathfrak{K}_{er}=&g\beta\mathbf{H}_{er}\cdot\sum_j\mathbf{I}_j+\sum_{k>j}(A_{jk}\mathbf{I}_j\cdot\mathbf{I}_k+B_{jk}I_{jz}I_{kz})\\
&+\sum_{j',k}C_{j'k}I_{j'z}I_{kz}\\
&+\sum_{k'>j'}A_{j'k'}\mathbf{I}_{j'}\cdot\mathbf{I}_{k'}+B_{j'k'}I_{j'z}I_{k'z}\\
&+g'\beta[H_0\mathbf{k}_r-(\omega/\gamma')\mathbf{i}_r+H_1\mathbf{k}_r]\cdot\sum_{j'}\mathbf{I}_{j'},\qquad (53)
\end{aligned}$$

Here g' and γ' are respectively the g factor and gyromagnetic ratio of the primed ingredient, $A_{j'k'}$ and $B_{j'k'}$ are given by (22) and (23) and

$$C_{jk'}=\tilde{A}_{jk'}+(1-3\xi_{jk'}{}^2)gg'\beta^2r_{jk'}{}^{-3}.\qquad (54)$$

In (53) we have neglected time-dependent terms as before. We can also neglect the term $g'\beta H_1 \sum I_{j'x}$ which is nonsecular if $|\omega - \gamma' H_0|$ is much greater than the resonance line width of the unprimed nuclei. The term involving $\sum I_{j'z}$ then commutes with the rest of the Hamiltonian and can be ignored, since the unprimed spins are not affected directly by the rf field.

The remaining terms of the Hamiltonian are secular perturbations and do not commute with each other. This means that they are coupled together, with the rather surprising result that effective energy can be transferred from the unprimed system to the primed system. When rf energy is absorbed by the unprimed spins, part of this energy will be transferred to the primed system via the interaction $\sum C_{jk'} I_{jz} I_{k'z}$. This energy will be entirely in the form of spin-spin (internal) energy; the external energy of the primed spins (expectation value of the last term of $\mathfrak{K}_{er}$) will be unchanged. The average populations of the primed spin levels will remain at their equilibrium values, but the primed spins will become more ordered in orientation with respect to their local fields.

The statements in the previous paragraph may appear to contradict the usual assumption that two different nuclear magnetic ingredients in a solid interact entirely independently with the rf field, from which it would follow that the primed system is unaffected by rf power at the resonant frequency of the unprimed system. Actually this assumption is not quite true, since the spin-spin energy of the primed system evidently increases in this case. For most purposes this energy is negligibly small compared to the external energy (in the fixed system) of the primed system, which is unaffected by the rf field. Only in the present case, where effective energy is the important quantity, will the spin-spin energy be important, and then only in determining the behavior of the unprimed nuclei.

As before we assume that at high rf levels the spin system is in a canonical distribution of states with respect to the retained parts (all but the last term) of the effectively time-independent transformed Hamiltonian $\mathfrak{K}_{er}$. As a consequence of this assumption, the part of the nuclear magnetization due to the unprimed spins is in the effective field direction with magnitude M_{zp} while that due to the primed spins remains at its thermal equilibrium value in the z-direction.

The effect of the unlike neighbors can be expressed in terms of the ratio $(\delta H)^2/H_{er}^2$ of internal spin-spin energy to external (unprimed) spin energy. In Appendix C it is shown that

$$(\delta H)^2 = \tfrac{1}{3}\langle(\Delta H)^2\rangle_u + I(I+1)(fN\hbar^2\gamma^2)^{-1}$$
$$\times (\sum_{j\neq k}\tilde{A}_{jk} + \sum_{j'\neq k'}\tilde{A}_{j'k'}) + \langle(\Delta H)^2\rangle_{pu}$$
$$+ \tfrac{1}{3}(f'/f)\langle(\Delta H)^2\rangle_p, \quad (55)$$

where $\langle(\Delta H)^2\rangle_u$ is the contribution of the unprimed ingredient to the second moment[25] of its resonance, $\langle(\Delta H)^2\rangle_{pu}$ is the contribution of the primed magnetic

ingredient to the second moment of the unprimed resonance, $\langle(\Delta H)^2\rangle_p$ is the contribution of the primed ingredient to the second moment of the primed resonance, N is the total number of both ingredients, and fN and $f'N$ are the numbers of unprimed and primed nuclei respectively.

If the relaxation times of the two types of nuclei are equal the quasistatic equilibrium value M_{0p} of the unprimed magnetization M_{zp} is given by (38) using the same reasoning as before, with χ_0 taken to be the unprimed contribution to the static susceptibility. If the relaxation times of the unprimed and primed nuclei are T_1 and T_1', then it can be shown (Appendix C) that

$$M_{0p} = M_0 \cos\Theta\{1 + H_{er}^{-2}[2(\delta H)^2_u + 2(\delta H)^2_p T_1/T_1'$$
$$+ \langle(\Delta H)^2\rangle_{pu}(1 + T_1/T_1')]\}^{-1}, \quad (56)$$

where $(\delta H)^2_u$ is equal to the first two terms of $(\delta H)^2$ [Eq. (55)], $(\delta H)^2_p$ equals the third and fifth terms of $(\delta H)^2$, and M_0 is the unprimed contribution to the static equilibrium magnetization.

As before, the theory is valid only for rf field levels above saturation, and if the spin-lattice interaction results in correlated scattering for neighboring spins the remarks at the end of Sec. III(c) apply.

The predicted behavior of χ'' and $\partial\chi'/\partial H_0$ at resonance for a crystal with two magnetic ingredients is shown in Fig. 6. The absorption is as before, except that $g(\nu_0)$ may be different and the parameters of the saturation curve refer only to the unprimed nuclei. The predicted dispersion shown is that for a crystal in which the observed (unprimed) nuclei are in the minority, the relaxation times T_1 and T_1' are comparable, and the absorption is gaussian below saturation. The plateau in $\partial\chi'/\partial H_0$ above saturation is reduced relative to that for the pure case (curve a) because of the additional spin-spin interaction of the unlike nuclei. The line shape above saturation is the same as for one magnetic ingredient, with a suitable increase in $(\delta H)^2$.

E. Fast and Intermediate Modulation

When the period of the magnetic field modulation becomes comparable to the spin-lattice relaxation time the observed absorption and dispersion signals above saturation will differ from those obtained if T_1 is very short. The same remark applies if the rf amplitude or frequency is modulated. In solids it is difficult to avoid modulation effects because, except for the heavier metals, the nuclear relaxation time at 300°K is greater than 10 milliseconds, requiring modulation frequencies ω_m of 10 cps or less. Such low modulation frequencies are seldom used in practice, because of noise and stability considerations. This is evidently why the nonsaturation of the dispersion reported here has not been previously observed.

Another reason for considering fast modulation is that by so doing it is possible to obtain the spin lattice relaxation time. This possibility has been exploited by

Halbach,[18] who has developed the theory of fast magnetic field modulation for systems obeying the Bloch equations.

Theories[5,6] of fast modulation based on the assumption of a spin temperature lead to incorrect results, even for systems obeying the Bloch equations. In these theories it is assumed that, for $\omega_m T_1 \gg 1$, the spin temperature is that corresponding to the average values of H_0, H_1, and ω. Actually, for $T_1^{-1} \ll \omega_m \ll \gamma H_1$ the nuclear magnetization will remain in the direction of the effective field, and thus its z-component and temperature will vary sinusoidally with the z-component of the effective field.

In this section we treat only modulation of the magnetic field H_0. Frequency modulation of the rf field is equivalent, and amplitude modulation of H_1 can be treated similarly. We assume that $\omega_m \ll \gamma H_1$ and that ω_m is much smaller than the unsaturated line width, so that modulation effects of the type considered by Karplus[34] are negligible.

The applied magnetic field is

$$H = (\bar{H}_0 + H_m \cos\omega_m t)\mathbf{k} + (2H_1 \cos\omega t)\mathbf{i}. \qquad (57)$$

In addition to the explicit time dependence of H in (57), ω also increases or decreases very slowly in time as the spectrometer sweeps through the resonance line.

In general the x-component of magnetization is (to first order)

$$M_x = (M_x' + M_{x1}' \cos\omega_m t + M_{x2}' \sin\omega_m t) \cos\omega t$$
$$+ (M_x'' + M_{x1}'' \cos\omega_m t + M_{x2}'' \sin\omega_m t) \sin\omega t, \qquad (58)$$

where M_x', M_{x1}', etc. are constant in time (or vary only very slowly as ω is varied).

The apparent dispersion derivatives are defined as

$$\partial\chi_1'/\partial H_0 = M_{x1}'/2H_1 H_m, \qquad (59a)$$

$$\partial\chi_2'/\partial H_0 = M_{x2}'/2H_1 H_m, \qquad (59b)$$

$$\partial\chi_1''/\partial H_0 = M_{x1}''/2H_1 H_m, \qquad (59c)$$

$$\partial\chi_2''/\partial H_0 = M_{x2}''/2H_1 H_m. \qquad (59d)$$

$\partial\chi_1'/\partial H_0$ and $\partial\chi_1''/\partial H_0$ are the apparent dispersion and absorption derivatives observed when the lock-in detector is adjusted in phase with the modulation, and $\partial\chi_2'/\partial H_0$ and $\partial\chi_2''/\partial H_0$ are the apparent dispersion and absorption derivatives observed when the lock-in detector is adjusted 90° out of phase (in quadrature) with the modulation.

The Hamiltonian is transformed to a rotating system as before, but Θ and H_{er} depend on time sinusoidally with frequency ω_m. This frequency is so low that it induces no appreciable transitions between the eigenstates of $\mathcal{3C}_{er}$, and it can be regarded as a reversible adiabatic (slow) perturbation of the spin system (not the whole system, as $\omega_m T_1 \gtrsim 1$). It is then reasonable to assume as before that the spin system remains in its

highest entropy macrostate; i.e., in a canonical distribution of states.

In Appendix B it is shown that this assumption leads to the equation (for one magnetic ingredient)

$$\frac{d}{dt}\langle\langle\mathcal{3C}_{er}\rangle\rangle = \frac{d}{dt}\langle\langle\mathcal{3C}_{ep}\rangle\rangle = \frac{M_{zp}H_{er}}{T_1} - \frac{2\langle\langle\mathcal{3C}_{SS}\rangle\rangle}{T_1}$$
$$- \frac{M_0 \cos\Theta H_{er}}{T_1} - \mathbf{M}_r \cdot \frac{\partial\mathbf{H}_{er}}{\partial t}. \qquad (60)$$

Using (32) gives

$$\frac{d}{dt}\langle\langle\mathcal{3C}_{SS}\rangle\rangle = \frac{(+M_{zp}H_{er} - M_0 \cos\Theta H_{er} - 2\langle\langle\mathcal{3C}_{SS}\rangle\rangle)}{T_1}$$
$$+ \frac{\partial\mathbf{M}_r}{\partial t} \cdot \mathbf{H}_{er}. \qquad (61)$$

Equation (60) also follows directly from the first law of thermodynamics[35] for the transformed Hamiltonian $dU_{er}' = dQ_{er} + \mathbf{M}_r \cdot d\mathbf{H}_{er}$, where U_{er}' is the effective energy of the spin system $\langle\langle\mathcal{3C}_{er}\rangle\rangle$, and Q_{er} is the effective heat transferred from the lattice to the spin system via the spin-lattice interaction. Application of thermodynamics to $\mathcal{3C}_{er}$ is valid because the changes in $\mathcal{3C}_{er}$ are reversible (slow) and the coupling to the lattice is assumed weak.

The assumption of a canonical distribution of states implies as before that the magnetization is in the direction of $\mathbf{H}_{er}$ with magnitude M_{zp}, and that $\langle\langle\mathcal{3C}_{SS}\rangle\rangle = -M_z[(\delta H)^2/H_{er}]$. Substituting into (61) we get

$$\dot{M}_{zp} = -(M_{zp} - M_{0p})/T_{1p}$$
$$+ M_{zp}\dot{H}_{er}H_{er}^{-1}[1 + H_{er}^2/(\delta H)^2]^{-1}, \qquad (62)$$

where

$$T_{1p} = T_1[1 + (\delta H)^2/H_{er}^2][1 + 2(\delta H)^2/H_{er}^2]^{-1}, \qquad (63)$$

and M_{0p} is given by (38).

Similar reasoning shows that when two magnetic ingredients are present (62) still holds, and M_{0p} and T_{1p} are given by (48) and (56). If the spin-lattice relaxation is correlated between neighbors the considerations at the end of Sec. III(c) apply, and T_{1p} is the same quantity introduced there. M_{0p} is again given by (48) and T_{1p} can be empirically determined as described below.

If T_{1p} is large compared to the time taken to sweep through the entire resonance, we can neglect the term $(M_{zp} - M_{0p})/T_{1p}$ in (62). Assuming that initially ω is well off resonance ($|H_0 - \omega/\gamma| \gg \delta H, H_1$) and $\pm M_{zp} \simeq M_z = M_0$, we get

$$M_{zp} = \frac{\pm M_0}{[1 + (\delta H)^2/H_{er}^2]^{\frac{1}{2}}}, \qquad (64)$$

[34] R. Karplus, Phys. Rev. 73, 1020 (1948).

[35] W. P. Allis and M. A. Herlin, *Thermodynamics and Statistical Mechanics* (McGraw-Hill Book Company, Inc., New York, 1952), Eq. (48-5).

and

$$\partial\chi_1'/\partial H_0 = \pm\partial/\partial H_0 \frac{M_0\sin\Theta/2H_1}{[1+(\delta H)^2/H_{er}^2]^{\frac{3}{2}}}, \quad (65)$$

$$\partial\chi_2'/\partial H_0 \simeq \partial\chi_1''/\partial H_0 \simeq \partial\chi_2''/\partial H_0 \simeq 0. \quad (66)$$

The plus or minus sign in (64) and (65) depends on whether ω is initially less or greater than the resonance frequency. This is the case Bloch[4] calls adiabatic fast passage. The present analysis shows that to observe a fast passage signal it is not necessary to sweep through the resonance in a time short compared to T_2, as previously supposed,[4] but only in time short compared to T_1. In the case of solids, where $T_1 \gg T_2$, this makes observation of fast passage signals much easier. It is, of course, still necessary to use rf levels well above the saturation level.

If $T_{1\rho} \cong T_1$ is short compared to the time taken to pass through resonance, we can regard ω as fixed, and the first-order solution of (62) is

$$M_{z\rho} = \bar{M}_{0\rho} + M_1\cos\omega_m t + M_2\sin\omega_m t, \quad (67)$$

where $\bar{M}_{0\rho}$ is the quasi-steady-state value of $M_{z\rho} = M_{0\rho}$ corresponding to $H_0 = \bar{H}_0$. M_1 and M_2 are given by

$$M_1 = -(1+1/\omega_m^2 T_{1\rho}^2)^{-1}$$
$$\times\left(\frac{\bar{M}_{0\rho}H_m\cos\Theta}{H_{er}[1+H_{er}^2/(\delta H)^2]} - \frac{H_m}{\omega_m^2 T_{1\rho}^2}\frac{\partial M_{0\rho}}{\partial H_0}\right), \quad (68)$$

$$M_2 = \frac{1}{\omega_m T_{1\rho}}\left(-M_1 + H_m\frac{\partial M_{0\rho}}{\partial H_0}\right). \quad (69)$$

Here $\partial M_{0\rho}/\partial H_0$ is evaluated for $H_0 = \bar{H}_0$. (68) and (69) are obtained by substituting (67) into (62) and setting $M_{0\rho} = (H_m\cos\omega_m t)\,\partial M_{0\rho}/\partial H_0 + \bar{M}_{0\rho}$.

The apparent dispersion derivatives are [from Eqs. (33), (58), (59), and (67)]

$$\partial\chi_1'/\partial H_0 = M_1'\sin\Theta/2H_1 H_m$$
$$-\bar{M}_{0\rho}\sin^2\Theta\cos\Theta/2H_1^2, \quad (70)$$

$$\partial\chi_2'/\partial H_0 = M_2'\sin\Theta/2H_1 H_m. \quad (71)$$

At resonance,

$$\partial\chi_1'/\partial H_0 = (1+\omega_m^2 T_{1\rho}^2)^{-1}\partial\chi'/\partial H_0, \quad (72)$$

$$\partial\chi_2'/\partial H_0 = \omega_m T_{1\rho}\partial\chi_1'/\partial H_0. \quad (73)$$

Here $\partial\chi'/\partial H_0$ is the true dispersion derivative at resonance in the limit of slow modulation. Equation (73) shows that the relaxation time $T_{1\rho}$ can be experimentally determined from the ratio of the in-phase to the quadrature dispersion signals, and the true dispersion derivative can be calculated from (72). This method of measuring the relaxation time was previously suggested and applied to liquids by Halbach.[18] Similar effects have evidently also been observed by Portis and Shaltiel.[36] It

[36] A. M. Portis and D. Shaltiel, Phys. Rev. 98, 264(A) (1955).

will be noted that the relaxation times can also be measured by modulating the rf power level, as is sometimes more convenient for microwave studies of paramagnetic relaxation.

The apparent absorption derivatives are obtained from conservation of energy considerations in the fixed coordinate system. The rate of transfer of energy from the spins to the lattice is to a good approximation $H_0(M_0-M_z)/T_1$. Conservation of energy[35] for the spin system then requires that

$$\frac{d}{dt}\langle\langle\mathcal{3C}_s\rangle\rangle = -H_0(M_0-M_z)/T_1 - \mathbf{M}\cdot\frac{\partial\mathbf{B}}{\partial t}. \quad (74)$$

Using the fact that $\langle\langle\mathcal{3C}_s\rangle\rangle \simeq H_0 M_z$ and $\partial\mathbf{B}/\partial t \simeq \partial\mathbf{H}/\partial t$, and averaging over one rf period, we get

$$H_0(M_0-M_z)/T_1$$
$$= -\omega H_1(M_z'' + M_{x1}''\cos\omega_m t$$
$$+ M_{x2}''\sin\omega_m t) + H_0\dot{M}_z. \quad (75)$$

Equations (33), (58), (59), and (75) can be solved for the apparent absorption derivatives. The result is complicated and will be omitted. The absorption signal depends on both the modulation frequency and phase. Since it is not customary to adjust a lock-in detector with extreme care, the phase of the observed signal in previous measurements of T_1 by saturation must be regarded as uncertain, and the reported values of T_1 correspondingly uncertain. The resulting errors in T_1 are not likely to be greater than a factor of two or three because the onset of saturation will still occur at level $H_1 \simeq 2[\gamma^2 T_1 g(\nu_0)]^{-\frac{1}{2}}$ corresponding to the point where the rf transition probability is comparable to the spin-lattice transition probability. Fast modulation will only change the details of the absorption saturation and apparent asymptotic absorption at resonance for large H_1.

The predicted dependence of $T_{1\rho}$ on rf field is shown in Fig. 6, assuming uncorrelated spin-lattice relaxation between neighbors. In the limit of large H_1, $T_{1\rho}$ equals T_1 (or more generally T_{2e}; here we assume as usual $T_1 = T_{2e}$). At the value of H_1 corresponding to the knee of the dispersion curve $T_{1\rho}$ undergoes a transition to $T_1/2$ for a single magnetic ingredient, or to some other value for two magnetic ingredients as indicated by (48) and (56). Below saturation the observed dispersion signal is expected to be in phase with the modulation and to correspond to the true dispersion derivative. The observed $T_{1\rho}$ as defined by (73) is then expected to decrease in some unpredicted way corresponding to the dotted lines in Fig. 6.

IV. COMPARISON WITH EXPERIMENT

We have not made a detailed analysis of the observed line shapes, but it appears that they are in agreement with the predictions of the theory. In the metals the absorption and dispersion derivatives above saturation

are very nearly Lorentzian[20] and have the expected width. The apparent dispersion derivatives in NaCl at large rf fields appear to be in agreement with the theory, assuming $\omega_m T_1 \gg 1$ and, for the impure NaCl, assuming T_1 short compared to the few minutes taken to sweep through the resonance, or, for the Harshaw NaCl, assuming T_1 comparable to the time taken to sweep through the resonance.

The observation of the adiabatic fast passage[4] signal in the Harshaw NaCl is evidence that we were justified in neglecting the time-dependent terms in $\mathfrak{IC}_{er}$ and $\mathfrak{IC}_{e\rho}$ [Eqs. (20) and (21)]. If these terms could induce transitions among the different eigenstates of the time-independent part of the transformed Hamiltonian then the magnetization in the z_ρ-direction, $M_{z\rho}$, would be destroyed when ω passed through resonance. The observations on the Harshaw NaCl indicate that the relaxation time of $M_{z\rho}$ produced by these terms is greater than about one minute, so that they can be neglected for most purposes.

We now reconsider the absorption data of Fig. 1. In the limit of large H_1, (43) indicates that χ'' should approach $\chi_0 H_0 / 2T_1\gamma H_1^2$. In the limit of small H_1 the Kronig-Kramers relations indicate that χ'' should approach $\frac{1}{2}\pi\chi_0\nu_0 g(\nu)$, where $g(\nu)$ is the normalized unsaturated line shape. An attempt has been made to draw these asymptotes for the data of Fig. 1. The asymptotes should cross at the value of H_1 given by $\frac{1}{2}\gamma^2 H_1^2 T_1 g(\nu_0) = 1$. In this way we get 5.5 milliseconds for T_1 in aluminum and 3.55 for copper. Since it is uncertain whether the asymptotes drawn in Fig. 1 are the true ones these values of T_1 must be regarded as upper limits. In addition, inaccuracies in the absorption data may introduce as much as 20 percent error in T_1. These values of T_1 are not necessarily more reliable than those obtained in Sec. II, and do not appreciably alter the conclusions reached there concerning the electronic structure. They lead to values of $v_0 P_F m^*/m$ of 220 for aluminum and 240 for copper.

The dispersion data of Figs. 2 and 3, together with (72) and (73), yield values of the true dispersion
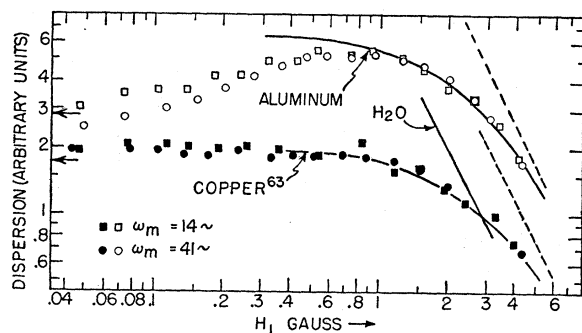

FIG. 7. Slow passage dispersion derivatives at resonance per resonated nucleus, as a function of rf power, inferred from the data of Figs. 2 and 3. The units of $N^{-1}\partial\chi'/\partial H_0$ are the same as in Figs. 2 and 3.

derivative contribution per nucleus shown in Fig. 7. Also shown in Fig. 7 is the relative dispersion derivative per proton for protons in water doped with paramagnetic impurity. This is the same H_2O line shown in Figs. 2 and 3. To get the absolute magnitude of $N^{-1}\partial\chi'/\partial H_0$ for comparison with experiment we can use either the H_2O data or the aluminum or copper dispersion derivative below saturation as a calibration.

In order to use the proton dispersion as a calibration it is necessary to assume a value of T_{2H}/T_{1H} in (5). Wangsness and Bloch[22] predict that this ratio is unity for protons in water relaxed by paramagnetic impurities, as considered here. The same result follows[32,37] from a somewhat more general theory of Kubo and Tomita.[23] Solomon[37] has recently measured T_{1H} and T_{2H}, using spin echo techniques for protons in water containing Fe ions. For Fe concentrations up to that required to reduce T_1 to one millisecond he finds that $T_{1H}/T_{2H} = 1.0 \pm 0.03$, in agreement with theory. Unfortunately the dispersion derivative observed in water in Fig. 7 is inconsistent with that observed below saturation in copper and aluminum (which is rigorously determined by the Kronig-Kramers relations and the unsaturated absorption line shape) unless we assume $T_{1H}/T_{2H} \simeq 2$. Thus it appears that either the errors in the data are greater than the conservative estimate of ± 20 percent, or that there is something wrong with the theory of nuclear resonance in liquids. The latter possibility should not be taken too seriously in view of the rather preliminary nature of the data, but it may be that the high concentration of paramagnetic impurities ($\simeq 1$ percent) could cause a decrease in the intensity of the dispersion signal because the rms value of the rapidly fluctuating local fields seen by the nuclei is larger than the applied field H_0.

In view of this difficulty we adopt the less accurate (but theoretically more rigorous) alternative of using the dispersion signal in aluminum and copper below saturation as a calibration. We approximate the line shape with an inverted truncated parabola:

$$g(\nu) = 3a^{-3}(a^2-\nu^2)/2 \quad \text{for} \quad \nu^2 < a^2,$$
$$g(\nu) = 0 \quad \quad \quad \text{for} \quad \nu^2 > a^2. \tag{76}$$

This is an excellent approximation for aluminum and a fair one for copper, which has a more nearly Gaussian resonance line than aluminum. Inserting (76) into the Kronig-Kramers relations and evaluating the second moment leads to

$$\partial\chi'/\partial H_0 = 0.3\chi_0 H_0 / \langle(\Delta H)^2\rangle_{Av}, \tag{77}$$

or

$$N^{-1}\partial\chi'/\partial H_0 = 0.6\pi I(I+1)\nu_0\gamma/3kT\langle(\Delta H)^2\rangle_{Av}, \tag{78}$$

where $\langle(\Delta H)^2\rangle_{Av}$ is the second moment of the line. If the line were assumed to be Gaussian the factor in (78) would be 1.0 instead of 0.6. In copper (78) predicts a

---

[37] I. Solomon (private communication). We are indebted to Dr. Solomon for permission to quote him prior to publication.

dispersion derivative which is expected to be slightly too small, because of the more nearly Gaussian shape of the copper resonance.

In aluminum the predicted second moment $\langle(\Delta H)^2\rangle_{Av}$ is 7.5 gauss,[2] neglecting possible anisotropic electronic coupling[26] between nuclei. Gutowski and McGarvey[1] report an experimental value of 10.5 gauss[2] and Rowland[38] a value of 8.7 gauss.[2] We assume a value of 9 gauss.[2] In copper Gutowski and McGarvey[1] report that experimentally $\langle(\Delta H)^2\rangle_{Av}$ is 6.3 gauss,[2] in reasonable agreement with their theoretical prediction of 5.6 gauss.[2] We use their experimental value. Corrections[1] to $\langle(\Delta H)^2\rangle_{Av}$ which depend on T_1 are negligible compared to the other approximations and uncertainties in the theory.

We use the aluminum dispersion derivative as a primary calibration, and assume that its experimental value (upper horizontal arrow in Fig. 7) is given correctly by (78). The copper dispersion derivative below saturation is then somewhat greater than the prediction of (78) (lower horizontal arrow), as expected. The discrepancies between the experimental points for aluminum at small H_1 are almost certainly due to experimental error.

The dotted lines in Fig. 7 are the predicted high rf field asymptotes for the dispersion derivatives, again using the low rf field aluminum dispersion as a calibration. The predicted asymptote is $N^{-1}\partial\chi'/\partial H_0 \rightarrow \chi_0 H_0/2NH_1^2$, as obtained from either (10) or (41), assuming $T_1 = T_{2e}$. The solid curves in Fig. 7 for large H_1 correspond to the prediction of (41), taking $(\delta H)^2 = 3.4$ gauss[2] for aluminum and 5.0 gauss[2] for copper. In aluminum the plateau predicted for $\partial\chi'/\partial H_0$ at intermediate fields is not resolved, owing to the relatively small ratio of T_1 to $(\gamma\delta H)^{-1}$ compared to that assumed for the predictions of Fig. 6. In copper the plateau evidently nearly coincides with the value of $\partial\chi'/\partial H_0$ below saturation.

In Fig. 8 are plotted experimental values of $T_{1\rho}$ obtained from (73) and the data of Figs. 2 and 3. For large H_1 the observed $T_{1\rho}$ values agree fortuitously well with the values of T_1 obtained in the beginning of this section, and disagree with the values of T_1 in Table I.

The behavior of $T_{1\rho}$ is in conflict with (63), which is based on the assumption of incoherent relaxation of neighboring nuclei implicit in (35). If this assumption were correct $T_{1\rho}$ should reach a plateau of about $\frac{1}{2}T_{1\rho}$ at the value of $H_1(\simeq 1$ gauss) at which the intermediate plateau of the dispersion derivative occurs. Such a plateau apparently exists but the value of $T_{1\rho}$ is too large. Such a large discrepancy cannot be explained by coherent nuclear relaxation unless the electronic band structure is appreciably different from the free electron

approximation with one electron per atom. We do not know the reason for this behavior.

Since the discrepancy in $T_{1\rho}$ is evidently real, at least in the case of copper, we are forced to use the more empirical approach described at the end of Sec. III. For $H_1 \gtrsim 1$ gauss, $T_{1\rho}$ can be approximated by

$$T_{2e}[1+(\delta H)^2/H_1^2][1+\alpha(\delta H)^2/H_1^2]^{-1}, \qquad (79)$$

where T_{2e} is 5.5 milliseconds for aluminum and 3.55 milliseconds for copper, and α is 1.7 for aluminum and 1.3 for copper. T_{2e} is used in (79) because $T_{1\rho}$ is expected to approach T_{2e}, the transverse spin-lattice relaxation time, in the limit of large H_1 and at resonance.

If we assume that $T_1 = T_{2e}$ as would be indicated by the values of T_1 obtained at the beginning of this section, (49) predicts the same dependence of $\partial\chi'/\partial H_0$ as before (solid lines in Fig. 7) if we take $(\delta H)^2 = 4$ gauss[2] for aluminum and 7.7 gauss[2] for copper.

A third interpretation of the data obtains if we assume that the values of T_1 in Table I are correct. This assumption is in conflict with the prediction[13,22] $T_1 = T_{2e}$ for a nucleus in a Fermi gas of electrons. The predicted asymptote of $\partial\chi'/\partial H_0$ is increased by T_{2e}/T_1 and (41) is in reasonable agreement with the data if we take $(\delta H)^2 = 5.9$ gauss[2] for aluminum and 10 gauss[2] for copper.

We now estimate the theoretical value of $(\delta H)^2$. If we assume $\tilde{A}_{jk} = 0$, $(\delta H)^2$ is predicted by (31) and (55) to be 2.5 to 3 gauss[2] for aluminum and 2.85 to 3.1 gauss[2] for copper. The lower limits of these estimates correspond to the classical dipolar interaction between nuclei and the upper limits correspond to the fact that the observed[1,39] second moments of the resonance line are ten to twenty percent larger than their theoretical values, possibly because of additional psuedo-dipolar[26] coupling between nuclei via the conduction electrons.

It is clear that the observed values of $(\delta H)^2$ cannot be explained by classical dipolar coupling alone. Ruderman and Kittel have calculated the magnitude of the exchange-type coupling between nuclei due to the conduction electrons; the result of their calculation can be
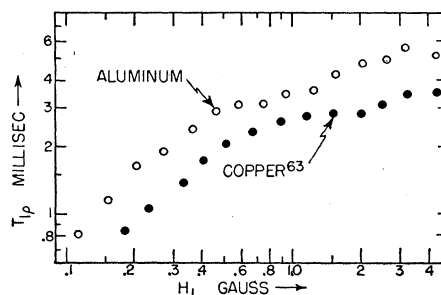

FIG. 8. The relaxation time $T_{1\rho}$ as obtained from the 41 cps data of Figs. 2 and 3.

[38] T. J. Rowland (private communication). This is the average value of two runs and is thought to be at least 10 percent accurate. The accuracy is difficult to estimate because of uncertainties in the wings of the line.

[39] K. Kambe, Phys. Rev. (to be published).

written [using Eq. (2)]:

$$\tilde{A}_{jk}=\frac{\hbar[2k_m r_{jk}\cos(2k_m r_{jk})-\sin(2k_m r_{jk})]}{8\pi^2 m^* r_{jk}^{-4}(T_{1j}T_{1k})^{\frac{1}{2}}kT}\left(\frac{\pi v_0}{3}\right)^{\frac{2}{3}}. \quad (80)$$

T_{1j} and T_{1k} are the relaxation times of nuclei j and k, and the relaxations represented by these times are assumed due only to the S-character of the electronic wave function near the Fermi surface; if the electronic P-character contributes to the relaxation (80) estimates too large a value for $\tilde{A}_{jk}$. To obtain (80) Ruderman and Kittel also assume that the electronic energy contours in k space are spherical, corresponding to an effective mass m^* and a wave number k_m at the Fermi level.

For $m^*=m$ and the values of T_1 in Table I, (80) predicts that $h^{-1}\tilde{A}_{jk}=80\sim$ for nearest neighbors in aluminum and $h^{-1}\tilde{A}_{jk}=140\sim$ for nearest Cu[63] neighbors in copper. These values lead to additional contributions to $(\delta H)^2$ due to nearest neighbors only of about 0.3 gauss^2 for both aluminum and copper. To agree with experiment we have to assume that $\tilde{A}_{jk}$ is about 2 times its theoretical value in aluminum, and about 3 times in copper. These factors are rather large, but might result from a small effective mass or a complex band structure. An exchange-type interaction of this magnitude might still be small enough to cause relatively little exchange narrowing of the unsaturated resonance, as is observed. Unfortunately for this interpretation, Kambe[38] has predicted theoretically that in copper $m^*\cong m$ so that an anomalously large $\tilde{A}_{jk}$ is not expected.

We may summarize this section by saying that the theory agrees fairly well with experiment provided we assume that the exchange-type coupling constant $\tilde{A}_{jk}$ is two or three times greater than its theoretical value, and that the relaxation of neighboring nuclear spins is coherent to a degree considerably greater than would be expected from simple considerations. These observations are consistent with the assumption of an almost filled or almost empty band with a small effective mass. There appears to be no independent support for such an assumption. If we assume instead a simple electronic structure with one electron per atom and $m^*=m$, the agreement between theory and experiment is not so good, but is considerably improved over that of previ-
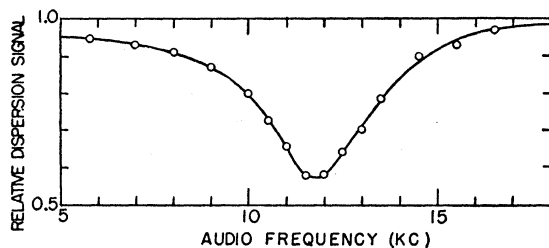
ous[4-6] theories of saturation as applied to solids. Finally, we should re-emphasize the fact that the interpretation of this section is based on a questionable calibration, owing to the disagreement of the proton calibration with the other data.

V. ROTARY SATURATION

The effect which we have called rotary saturation was suggested by the previous use of the rotating coordinate system representation. Much of the theory above will be useful in treating this effect in solids, but it is not necessary to understand Sec. III in order to understand rotary saturation, as it is also a consequence of the Bloch equations.

The effect is observed in a liquid obeying the Bloch equations as follows: the dispersion derivative signal is observed at resonance well above saturation, using a magnetic field modulation amplitude H_m which is a sizable fraction of the rf amplitude H_1, and a modulation period ω_m^{-1} much larger than T_1 and T_2 (or T_{2e} in the case of a solid). An audio-frequency magnetic field of frequency ω_a and amplitude[40] H_a, oriented in the z direction, is also applied to the sample. When the audio-frequency approaches the frequency

$$\omega_a=\gamma H_{er}\cong\gamma H_1, \quad (81)$$

the dispersion signal is observed to decrease, and it goes through a minimum when the condition (81) is satisfied. The frequency γH_{er} is the classical nutation frequency of the nuclei in the rf magnetic field.

Figure 9 shows a rotary saturation run obtained with water heavily doped with paramagnetic (Mn^{++}) ions. The dispersion minimum frequency of 12.75 kc corresponds to the proton resonance frequency in a field of 3.0 gauss. Search coil measurements indicated that in the run of Fig. 9, H_1 was 3 gauss within the probable experimental error; these measurements of H_1 were rather inaccurate because of the uncertain geometric factors involved. Actually the run of Fig. 9 was used to calibrate the rf field for use in the other runs reported in this paper, and the rf field in this run was therefore *assumed* to be 3.0 gauss. The theoretical justification for this assumption will be given below.

Rotary saturation can be understood by transforming to the rotating coordinate system. In Fig. 10(a) is shown H_{er} during a positive peak of the 14 cps magnetic field modulation. The Bloch equations predict that in the absence of the applied audio field and in the limit of large H_1 the magnetization will be approximately in the direction of H_{er} with a magnitude $M_{zp}=M_0\cos\Theta T_{2H}/T_{1H}$. At the negative peak of the modulation the situation depicted by the dotted arrows in Fig. 10(a) applies. The observed rf dispersion signal is proportional to M_{zp}.

The action of the audio field H_a in the rotating

FIG. 9. Rotary saturation run on protons in water heavily doped with manganese ions. H_1 was thought to be 3.0 gauss, H_a was about 0.6 gauss, and the magnetic field modulation was 1 gauss peak-to-peak.

---

[40] Throughout this paper, peak values of the audio magnetic field will be used.

coordinate system can be seen by analogy to ordinary saturation in the fixed coordinate system, Fig. 10b. If $\Theta \simeq 90°$ the correspondences $H_{er} \rightarrow H_0$, $M_{0\rho} \rightarrow M_0$, and $H_a \rightarrow 2H_1$ apply, and the spin relaxation processes are almost the same in the two coordinate systems (identical if $T_1 = T_2$ as is frequently the case). In ordinary saturation the rf field $2H_1$ reduces the amplitude of M_z to some value less than its equilibrium value M_0. In rotary saturation the audio field H_a reduces the amplitude of $M_{z\rho}$ to some value less than its quasi-static equilibrium value $M_{0\rho}$. As a consequence the observed dispersion signal is correspondingly reduced, as in Fig. 9. Power is also absorbed from the audio field, but this absorption is normally too small to observe directly.

Rotary saturation can also occur off resonance, for $|H_0 - \omega/\gamma| \simeq H_1$, although it is most directly observed at resonance. As before, the audio field is most effective in reducing the magnetization $M_{z\rho}$ and the dispersion signal when the condition $\omega_a = \gamma H_{er}$ is obeyed. The effectiveness of the audio field is reduced by a factor $\sin^2 \Theta$ since only the square of the component of $\mathbf{H}_a$ perpendicular to $\mathbf{H}_{er}$ acts in the double saturation. Some rather complicated dispersion derivative traces can be obtained by using various fixed values of ω_a
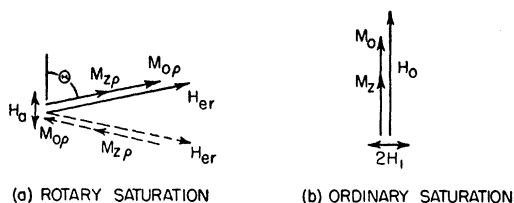

(a) ROTARY SATURATION   (b) ORDINARY SATURATION

FIG. 10. Explanation of rotary saturation.

greater than γH_1. These signals all appear to be consistent with this simple picture.

Rotary saturation can be treated theoretically in liquids by transforming to a doubly rotating coordinate system,[24] the first rotation being about H_0 at frequency ω, the second about H_{er} at frequency ω_a. We ignore the circularly polarized component of H_a which rotates at frequency $2\omega_a$ in the doubly rotating system, and we also ignore the time dependent parts of the relaxation terms (involving T_1 and T_2), which vary sinusoidally with frequency ω_a. The resulting expression for $M_{z\rho}$ is similar to that for M_z as predicted by the Bloch equations for ordinary saturation, with the substitutions (for $\Theta \simeq 90°$) $M_0 \rightarrow M_{0\rho}$, $H_0 \rightarrow H_{er}$, $2H_1 \rightarrow H_a$, $M_z \rightarrow M_{z\rho}$, $\omega \rightarrow \omega_a$, $T_1 \rightarrow T_2$, and $T_2^{-1} \rightarrow \frac{1}{2}(T_1^{-1} + T_2^{-1})$. Thus the minimum of $M_{z\rho}$ and the dispersion signal should indeed occur when $\omega_a = \gamma H_{er}$, which near resonance corresponds to $\omega_a = \gamma H_1$.

The time dependent parts of the transformed Bloch equations will introduce some error in this solution and are probably responsible for the asymmetry in the run of Fig. 9. They will probably not introduce more than a few percent error in the determination of H_1 by this method.
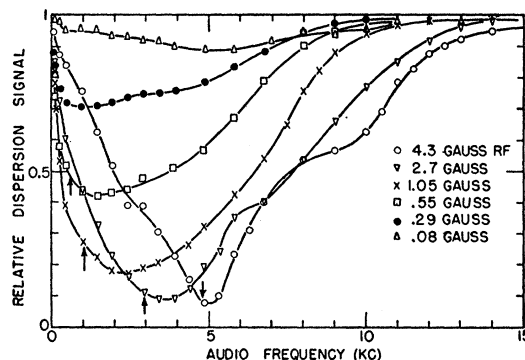

FIG. 11. Rotary saturation runs in pure aluminum. The audio amplitude H_a was about 2 gauss, the modulation amplitude was 2.5 gauss peak-to-peak, and the resonance frequency was about 7.6 megacycles. The arrows indicate the frequency $\gamma H_1/2\pi$ for the various runs.

In Fig. 11 are shown some rotary saturation runs in aluminum, for various values of H_1. In solids the line width is determined by the static dipolar interaction among different spins rather than by collision broadening as in the case of liquids. For low rf fields the dipolar interaction displaces the minimum to a frequency above γH_1 (indicated by arrows in Fig. 11), but for large H_1 the minimum very nearly coincides with the predicted nutation frequency.

Rotary saturation in solids can be treated theoretically in the rotating system in the same way that ordinary saturation was treated by BPP, because the analogy of Fig. 10 also applies to the case of solids. The effective[29] energy absorbed per second by the spins from the audio field is (for $\Theta \simeq 90°$)

$$\tfrac{1}{2}\omega \chi_a'' H_a^2, \tag{82}$$

where χ_a'' is the imaginary part of the audio susceptibility in the z, or x_ρ (approximately) direction. Since the system is assumed to be in a canonical distribution of states with respect to $\mathcal{3C}_{er}$, for small H_a, we can write

$$\chi_a'' = \tfrac{1}{4}\omega(M_{0\rho}/H_{er})f(\nu_a) \tag{83}$$

where $M_{0\rho}/H_{er}$ is the rotary analog of χ_0, and $f(\nu_a)$ is a normalized shape function similar to that defined by Broer.[41,42] (83) is consistent with a rotary version of the Kronig-Kramers relations and can be derived in the same way as the analogous equation for ordinary paramagnetic resonance.

The effective energy absorbed per unit time by the lattice from the spin system is [from Eqs. (37), (47), and (48)]

$$\left[\frac{\partial}{\partial t}\right]_{SL} \langle\langle \mathcal{3C}_{er}\rangle\rangle$$
$$= -(\langle\langle \mathcal{3C}_{er}\rangle\rangle - \langle\langle \mathcal{3C}_{er}\rangle\rangle_0)/T_{1\rho}$$
$$= (M_{z\rho} - M_{0\rho})H_{er}[1 + (\delta H)^2/H_{er}^2]/T_{1\rho}. \tag{84}$$

[41] L. J. F. Broer, thesis, Amsterdam, 1945 (unpublished); and Physica 10, 801 (1943).
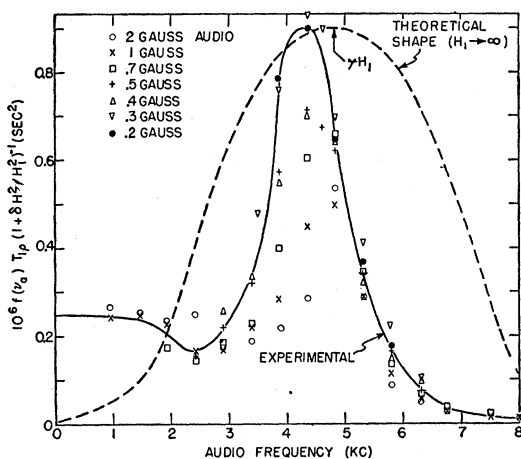[42] A. Wright, Phys. Rev. 76, 1826 (1949).

FIG. 12. Values of $f(\nu_a)T_{1\rho}[1+(\delta H)^2/H_1^2]^{-1}$ obtained from double saturation data for aluminum. H_1 was 4.3 gauss, the modulation was 2.5 gauss peak-to-peak, and ν_0 was about 7.6 megacycles. The arrow indicates the frequency $\gamma H_1/2\pi$.

Here $\langle\langle\mathcal{3C}_{er}\rangle\rangle_0=M_{0\rho}H_{er}[1+(\delta H)^2/H_{er}^2]$, the quasi-equilibrium value of $\langle\langle\mathcal{3C}_{er}\rangle\rangle$.

In the quasi-steady state the thermal rate of decrease of $\langle\langle\mathcal{3C}_{er}\rangle\rangle$ given by (84) must equal the rate at which (effective) energy is absorbed from the audio magnetic field, given by (82). If we assume, following BPP, that (83) holds under the substitution $M_{0\rho}\rightarrow M_{z\rho}$ in arbitrarily large H_a, we get

$$M_{z\rho}/M_{0\rho}=\{1+\tfrac{1}{2}H_a^2\omega_a^2f(\nu_a)T_{1\rho}H_{er}^{-2}$$
$$\times[1+(\delta H)^2/H_{er}^2]^{-1}\}^{-1}.\quad(85)$$

The observed rf susceptibility is thus reduced by a factor equal to the right-hand side of (85).

Actually, the assumption that $M_{z\rho}$ can be substituted for $M_{0\rho}$ in (83), for arbitrary H_a, is not justified. This is the same erroneous assumption made in the BPP theory[5] of ordinary saturation, as discussed in Sec. III(a). Equation (85) is expected to hold only for small H_a, where $M_{z\rho}/M_{0\rho}\approx1$.

The shape function $f(\nu_a)$ can be determined experimentally by making a series of runs at constant H_1 and different H_a and ω_a, and using (85) to determine $f(\nu_a)T_{1\rho}[1+(\delta H)^2/H_{er}^2]^{-1}$. Data obtained in this way for aluminum and copper are shown in Figs. 12 and 13. In drawing the experimental curve (solid line) through these data we have given the greatest weight to those points obtained at low audio power levels, since (85) is expected to be more accurate at these levels.

Integration of the solid curves in Figs. 12 and 13 yields values of $T_{1\rho}[1+(\delta H)^2/H_1^2]^{-1}$ of 5.6 milliseconds for copper and 2.2 milliseconds for aluminum. These times differ from values predicted from the previously estimated $T_{1\rho}$ and $(\delta H)^2$ by a factor of about two. The value for copper is too large and that for aluminum is too small. The reason for this discrepancy is not known.

We have not attempted to analyze the shape function $f(\nu_a)$ in detail, but we can make a few general remarks.

A considerable number of theoretical predictions concerning $f(\nu_a)$ can be made using the methods of Van Vleck[25] and Wright,[42] but the Hamiltonian $\mathcal{3C}_{er}$ has fewer secular terms than the spin Hamiltonian $\mathcal{3C}_S$ in the fixed coordinate system, and therefore the theoretical work of Wright[42] is not directly applicable here. As expected, $f(\nu_a)$ has definite peaks at zero frequency and at γH_1. The significance, if any, of the small departures of the resonant peaks from the value γH_1 is not known. These departures may be due in part to experimental error.

In the limit of large H_{er}, $f(\nu_a)$ is expected to be a symmetrical curve centered about the resonance frequency γH_1, and the moments of $f(\nu_a)$ in this case have been calculated by Van Vleck. It is noteworthy that if $\tilde{A}_{jk}=0$ the secular part of $\mathcal{3C}_{e\rho}$ [first three terms of Eq. (20)] contains a spin interaction identical in form and exactly half as large as the secular part of the Hamiltonian in the fixed coordinate system. This implies that $g(\nu)$, the rf line shape, should be exactly similar and twice as broad as $f(\nu_a)$. The expected shapes $f(\nu_a)\sim g(2\nu)$ are plotted in Figs. 12 and 13; here $g(\nu)$ was obtained experimentally. The observed $f(\nu_a)$ is considerably narrower than the predicted shape, which may be due in part to the fact that H_1 is not very large and is in fact comparable to the predicted line width. Another possible reason for the narrow observed $f(\nu_a)$ may be the terms $\tilde{A}_{jk}\mathbf{I}_j\cdot\mathbf{I}_k$, which are expected to produce exchange narrowing of $f(\nu_a)$. It is rather surprising that they do not also produce appreciable exchange narrowing of the rf resonance line.

It is amusing to note that if $1-3\cos^2\Theta=0$ and H_1 is large, the line width should be zero, except for a small spin-lattice relaxation broadening. In the case of the data of Figs. 12 and 13 the modulation was not large enough to induce such narrowing.

In conclusion we may say that besides providing an accurate calibration of the rf field, rotary saturation is a relatively simple way to study the properties of spin systems in small magnetic fields. This statement is based on the fact that the time dependent part of $\mathcal{3C}_{er}$ really can be neglected to a very good approximation, so that rotary saturation is really closely analogous to ordinary saturation.

VI. CONCLUDING REMARKS

The theory and experiment in this paper demonstrate the usefulness of the rotating coordinate representation in resonance problems. The rotating coordinate representation should be useful in treating other types of relaxation and spin interaction than those considered here. For example, the rotary saturation experiment indicates that the perturbations responsible for transverse (T_2 or T_{2e}) relaxation of nuclei are those of frequency γH_1, rather than zero frequency.

All the theory in this paper can, of course, be applied to paramagnetic resonance under suitable conditions. In the case of ferromagnetic resonance the approximations

made above are presumably invalid, but some progress might be made along similar lines.

An as yet unexploited consequence of this work is the feasibility of measuring spin temperatures and relaxation times and obtaining negative temperatures in solids by the method of adiabatic fast passage. The experimental technique would be similar to that employed by Drain[43] and others[44] to measure relaxation times in liquids.

The implications of this research concerning the interpretation of previous work are rather unimportant, except for the probable errors in previous fast modulation saturation measurements of T_1, as discussed in Sec. III. The optimum signal to noise ratio predicted by Bloch and BPP is too small by a factor of about T_2/T_1, provided the dispersion mode is observed under conditions of slow passage. This gain is usually offset by the additional apparatus noise at high rf power levels, and by the fact that T_1 is frequently so long that slow passage is impractical.

ACKNOWLEDGMENTS

APPENDIX A

The method used to calculate the ratio of the effective external energy $M_{z\rho}H_{er}$ to internal spin-spin effective energy is similar to that used by Van Vleck[31] to calculate the specific heat of a spin system. However, the form of the Hamiltonian is slightly different and the calculation is simplified by the use of the density matrix[21] formalism.

The assumption of a canonical distribution of states with respect to the transformed spin Hamiltonian is equivalent to the assumption that the state of the solid is described by the density matrix (in the r-rotating system)

$$\rho \cong C \exp(-\mathfrak{3C}_{er}/kT^* - \mathfrak{3C}_L/kT). \quad (86)$$

Here C is a normalizing factor making $\mathrm{Tr}\rho = 1$, T^* is a constant analogous to an effective spin temperature in the rotating system, $\mathfrak{3C}_L$ is the lattice (nonspin) Hamiltonian, and T is the lattice temperature. $\mathrm{Tr}O$ denotes the trace (diagonal sum) of the operator O. The spin-lattice interaction $\mathfrak{3C}_{SL}$ (or $\mathfrak{3C}_{SLR}$ transformed to the rotating coordinate system) is neglected since it is assumed to be small. The first term of the exponential (86) represents the assumption that the spin system is in a canonical distribution of states with respect to $\mathfrak{3C}_{er}$,

[43] L. E. Drain, Proc. Phys. Soc. (London) A26, 301 (1949).
[44] Ciaroti, Cristiani, Giulotto, and Lanzi, Nuovo cimento 12, 519 (1954).
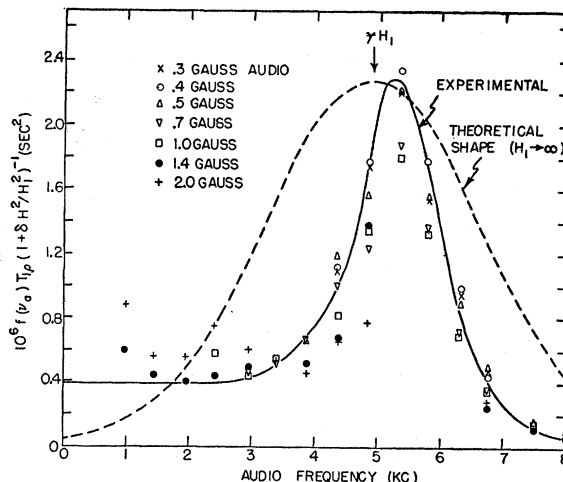

FIG. 13. Values of $f(\nu_a)T_{1\rho}[1+(\delta H)^2/H_1^2]^{-1}$ for Cu^{63} in annealed copper. The values of H_1, H_a, and modulation are the same as those in Fig. 12. The arrow indicates the frequency $\gamma H_1/2\pi$.

corresponding to the spin effective temperature T^*. The second term represents the assumption that the lattice (electrons, lattice vibrations, etc.) is relatively unaffected by the rf field and can be described by the temperature T.

In practice we can assume that T^* is large enough for us to write

$$\rho \cong (1 - \mathfrak{3C}_{er}/kT^*)\rho_L, \quad (87)$$

where

$$\rho_L = C \exp(-\mathfrak{3C}_L/kT). \quad (88)$$

The expectation value of $\mathfrak{3C}_{er}$ averaged over the canonical ensemble is

$$\langle\langle\mathfrak{3C}_{er}\rangle\rangle = \mathrm{Tr}\mathfrak{3C}_{er}\rho \cong (\mathrm{Tr}\mathfrak{3C}_{er}\rho_L - \mathrm{Tr}\mathfrak{3C}_{er}^2\rho_L/kT^*). \quad (89)$$

This expression is easily evaluated by using a representation in which the operators I_{jz} and $\mathfrak{3C}_L$ are diagonal. In this case we can write $C^{-1} = (2I+1)^N \mathrm{Tr}_L \times \exp(-\mathfrak{3C}_L/kT)$ where N is the total number of spins and $\mathrm{Tr}_L O$ denotes the diagonal sum of the operator O over all the eigenvalues $\mathcal{E}_L$ of $\mathfrak{3C}_L$, keeping the quantum numbers m_{Ij} (eigenvalues of I_{jz}) fixed. In the same representation we can write

$$\mathrm{Tr}\mathfrak{3C}_{er}^2\rho_L = (\mathrm{Tr}_I\mathfrak{3C}_{er}^2)(\mathrm{Tr}_L\rho_L), \quad (90)$$

where $\mathrm{Tr}_I\mathfrak{3C}_{er}^2$ denotes the diagonal sum of $\mathfrak{3C}_{er}^2$ over the quantum numbers m_{Ij}, keeping the quantum number $\mathcal{E}_L$ fixed. This relation follows directly from the diagonality of $\mathfrak{3C}_{er}$ with respect to the $\mathcal{E}_L$ and of $\mathfrak{3C}_L$ with respect to the m_{Ij}.

Using the easily verified relations:

$$\mathrm{Tr}_I I_{j\nu}I_{k\mu} = \tfrac{1}{3}I(I+1)(2I+1)^N\delta_{j,k}\delta_{\nu,\mu}, \quad (91)$$

$$\mathrm{Tr}_I I_{j\nu}I_{k\mu}I_{m\xi}I_{n\eta}$$
$$= (1/9)I^2(I+1)^2(2I+1)^N\delta_{i,k}\delta_{\mu,\nu}\delta_m,_n\delta_{\xi,\eta}, \quad (92)$$

where ν, μ, ξ, $\eta = x$, y, z and $j \neq m$, $k \neq n$, we can evaluate $\mathrm{Tr}\mathfrak{3C}_{er}^2\rho_L$ and similarly show that $\mathrm{Tr}\mathfrak{3C}_{er}\rho_L$ is zero. The

result is

$$-kT^*\langle\langle\mathfrak{K}_{er}\rangle\rangle=\tfrac{1}{3}Ng^2\beta^2H_{er}{}^2I(I+1)$$
$$+(1/9)I^2(I+1)^2\sum_{k>j}(3\tilde{A}_{jk}{}^2+\tfrac{2}{3}B_{jk}{}^2). \quad (93)$$

The first term of $\langle\langle\mathfrak{K}_{er}\rangle\rangle$ is the external energy $-\mathbf{M}_r\cdot\mathbf{H}_{er}$, as can be verified by directly calculating $\langle\langle\mathbf{M}_r\rangle\rangle$ $=\langle\langle g\beta\sum\mathbf{I}_j\rangle\rangle$ using (87). The second term is the internal spin-spin effective energy. Equations (30) and (31) follow directly from (93) on comparison with the Van Vleck[25] expression for $\langle(\Delta H)^2\rangle_{Av}$.

APPENDIX B

The equation of motion of $\langle\langle\mathfrak{K}_{er}\rangle\rangle$ is

$$\frac{d}{dt}\langle\langle\mathfrak{K}_{er}\rangle\rangle=\left\langle\left\langle\frac{i}{\hbar}[\mathfrak{K}_r,\mathfrak{K}_{er}]\right\rangle\right\rangle+\left\langle\left\langle\frac{\partial\mathfrak{K}_{er}}{\partial t}\right\rangle\right\rangle, \quad (94)$$

where $\mathfrak{K}_r$ is the total Hamiltonian $\mathfrak{K}=\mathfrak{K}_L+\mathfrak{K}_{SL}+\mathfrak{K}_S$ transformed to the r-system:

$$\mathfrak{K}_r=\mathfrak{K}_L+\mathfrak{K}_{SLR}(t)+\mathfrak{K}_{er}. \quad (95)$$

Since $\mathfrak{K}_{er}$ commutes with itself and $\mathfrak{K}_L$, (94) becomes

$$\frac{d}{dt}\langle\langle\mathfrak{K}_{er}\rangle\rangle=\langle\langle\partial\mathfrak{K}_{er}\rangle\rangle-\mathbf{M}_r\cdot\frac{\partial\mathbf{H}_{er}}{\partial t}. \quad (96)$$

The abbreviation ∂O is used for $-i\hbar^{-1}[\mathfrak{K}_{SLR},O]$, so that $\langle\langle\partial O\rangle\rangle$ is the time rate of change of the canonical average expectation value $\langle\langle O\rangle\rangle$ of O, due to the (time dependent) spin-lattice interaction $\mathfrak{K}_{SLR}$. In the treatment of fast or intermediate passage the first and last terms of (96) are retained [Eq. (65), Sec. III(e)], while under steady-state conditions they are by definition zero, and the second term is therefore also zero. $\langle\langle\partial\mathfrak{K}_{er}\rangle\rangle$ is also referred to in Sec. III as $[\partial/\partial t]_{SL}\langle\langle\mathfrak{K}_{er}\rangle\rangle$. Assuming that the spin-lattice interaction $\mathfrak{K}_{SL}$, and therefore the transformed interaction $\mathfrak{K}_{SLr}$, is linear in the operators I_{jx}, I_{jy}, I_{jz}, we get

$$\langle\langle\partial\mathfrak{K}_{er}\rangle\rangle=g\beta\sum_j\mathrm{Tr}(\partial\mathbf{I}_j)\cdot\mathbf{H}_{er}\,\rho$$
$$+g^2\beta^2\sum_{j\neq k}[A_{jk}{}^2\,\mathrm{Tr}(\partial\mathbf{I}_j)\cdot\mathbf{I}_k\,\rho$$
$$+B_{jk}{}^2\,\mathrm{Tr}(\partial I_{jz})I_{kz}\,\rho]. \quad (97)$$

In (97) ρ is understood to be given by (87).

To evaluate (97) we use the assumption (34), which in slightly more general form can be written

$$\mathrm{Tr}(\partial I_{jx})\rho'=-\mathrm{Tr}I_{jx}\,\rho'/T_{2e}, \quad (98a)$$

$$\mathrm{Tr}(\partial I_{jy})\rho'=-\mathrm{Tr}I_{jy}\,\rho'/T_{2e}, \quad (98b)$$

$$\mathrm{Tr}(\partial I_{jz})\rho'=-(\mathrm{Tr}I_{jz}\,\rho'-I_0)/T_1. \quad (98c)$$

Here we have temporarily abandoned the assumption $T_1=T_{2e}$, and ρ' is a density matrix describing an arbitrary state of the spin system. Thus $\rho'=\rho_I\rho_L$, where ρ_I is an arbitrary function of the spin operators for which $\mathrm{Tr}_I\rho_I=(2I+1)^N$. Use of the various operators 1, $1+I_{j\xi}$, $1+I_{j\xi}I_{k\eta}$, $1+I_{j\xi}I_{k\eta}I_{k\xi}$ (with ξ, η, $\zeta=x$, y, z, and

j, k and ξ, η, ζ not necessarily identical or nonidentical) for ρ_I yields

$$\mathrm{Tr}(\partial I_{jz})\rho_L=I_0/T_1, \quad (99)$$

$$\mathrm{Tr}(\partial I_{j\nu})I_{j\nu}\rho_L=-\tfrac{1}{3}I(I+1)/T_{2e}, \quad (100)$$

$$\mathrm{Tr}(\partial I_{jz})I_{jz}\rho_L=-\tfrac{1}{3}I(I+1)/T_1, \quad (101)$$

$$\mathrm{Tr}(\partial I_{jz})I_{jz}I_{k\nu}{}^2\rho_L=-(1/9)I^2(I+1)^2/T_1, \quad (102)$$

$$\mathrm{Tr}(\partial I_{j\nu})I_{j\nu}I_{k\mu}{}^2\rho_L=-(1/9)I^2(I+1)^2/T_{2e}, \quad (103)$$

where $j\neq k$; $\mu=x$, y, z; $\nu=x$, y. All other traces occurring in (97) are zero. Using these expressions we get

$$\langle\langle\partial\mathfrak{K}_{er}\rangle\rangle=Ng\beta\left(H_0-\frac{\omega}{\gamma}\right)\frac{I_0}{T_1}-\frac{Ng^2\beta^2I(I+1)}{3kT^*}$$

$$\times\left[\left(H_0-\frac{\omega}{\gamma}\right)^2\frac{1}{T_1}+\frac{H_1{}^2}{T_{2e}}\right]$$

$$+I^2(I+1)^2\sum_{j\neq k}\left\{-A_{jk}{}^2\left[\frac{1}{9T_1}+\frac{2}{9T_{2e}}\right]\right.$$

$$\left.-\frac{B_{jk}{}^2}{9T_1}-\frac{2A_{jk}B_{jk}}{9T_1}\right\}. \quad (104)$$

$\langle\langle\mathbf{M}_r\rangle\rangle=\mathrm{Tr}g\beta\sum_j\mathbf{I}_j\,\rho$ is easily shown to be a vector in the direction of $\mathbf{H}_{er}$ or $\mathbf{k}_\rho$, of magnitude

$$M_{z\rho}=I(I+1)g^2\beta^2NH_{er}/3kT^*. \quad (105)$$

The static equilibrium magnetization M_0 is given by the same formula with $M_{z\rho}\to M_0$, $T^*\to T$, and $H_{er}\to H_0$. Therefore (104) can be written

$$\langle\langle\partial\mathfrak{K}_{er}\rangle\rangle=-(M_{z\rho}-M_{0\rho})[1+(\delta H)^2/H_{er}{}^2]H_{er}/T_{1\rho}, \quad (106)$$

where

$$T_{1\rho}=\frac{M_{0\rho}[1+(\delta H)^2/H_{er}{}^2]T_1}{M_0\cos\Theta}, \quad (107)$$

and

$$M_{0\rho}=\frac{M_0\cos\Theta(T_1^{-1}\cos^2\Theta+T_{2e}^{-1}\sin^2\Theta)^{-1}}{T_1[1+\alpha(\delta H)^2/H_{er}{}^2]}. \quad (108)$$

If

$$\tilde{A}_{jk}=0, \quad \alpha=\left(\frac{16}{9T_1}+\frac{2}{9T_{2e}}\right)(T_1^{-1}\cos^2\Theta+T_{2e}^{-1}\sin^2\Theta)^{-1}.$$

If $T_{2e}=T_1$, and $\tilde{A}_{jk}$ is not necessarily zero, Eqs. (38) and (63) of Sec. III follow immediately.

In this calculation $\mathfrak{K}_{SL}$ and $\mathfrak{K}_{SLr}$ contain only the time dependent part of the spin-lattice interaction which is responsible for the relaxation, while $\mathfrak{K}_S$ and $\mathfrak{K}_{er}$ contain time independent parts which result from the spin-lattice interaction (i.e., chemical shift, Knight shift, and electron coupled spin-spin interactions).[26,27] As discussed in Sec. III(c), this procedure is hard to justify rigorously but seems reasonable physically.

APPENDIX C

We assume that the system is described by the density matrix

$$\rho = C \exp\{\mathfrak{K}_{er1}/kT^* + [g\beta H_0 \sum_{j'} I_{j'z} + \mathfrak{K}_L]/kT\}, \quad (109)$$

where $\mathfrak{K}_{er1}$ contains all the time-independent terms of $\mathfrak{K}_{er}$ [Eq. (53)] except the last. The reason for including all the spin-spin terms of $\mathfrak{K}_{er}$ is discussed in Sec. III(d).

The ratio of external unprimed spin energy to internal spin-spin energy is obtained by evaluating $\langle\langle \mathfrak{K}_{er1} \rangle\rangle$. Proceeding as in Appendix A, (55) easily follows.

The equation of motion of $\langle\langle \mathfrak{K}_{er1} \rangle\rangle$ is given by (96) with the substitutions $\mathfrak{K}_{er} \rightarrow \mathfrak{K}_{er1}$ and the density matrix (109) for that of (86). Evaluation of the various terms is similar to the procedure of Appendix B. Equations (99) to (103) hold for the substitutions $j \rightarrow j'$ and/or $k \rightarrow k'$ under suitable additional substitution of I_0', T_1', and T_{2e}'. (48) and (56) then follow easily from the assumption $T_1 = T_{2e}$ and $T_1' = T_{2e}'$.

Theory of Electroluminescence

W. W. PIPER AND F. E. WILLIAMS

General Electric Research Laboratory, Schenectady, New York

(Received February 11, 1955)

The theoretical basis for exciting luminescence by the application of an electric potential to a crystalline dielectric or semiconductor is considered. Three mechanisms of excitation are each shown to be theoretically feasible in appropriate solids and with suitable local field conditions: (1) the ionization of impurity systems directly by an electric field, (2) the acceleration of conduction electrons or positive holes in the valence band to kinetic energies sufficient to excite or ionize impurity systems or valence electrons by inelastic collisions, and (3) injection of charge carriers. Radiative de-excitation is feasible by two mechanisms: (a) direct recombination of conduction electrons and holes in the valence band, and (b) optical transitions characteristic of impurity systems known as activators. The characteristics of electroluminescence proceeding by these processes are examined theoretically.

INTRODUCTION

ELECTROLUMINESCENCE of various crystalline phosphors has been reported in the literature over a period of twenty-five years.[1-5] Various mechanisms have also been proposed.[2,3,5-7] In this paper the general mechanisms for converting an electrical potential applied to a crystal into luminescence will be examined theoretically. Previously considered mechanisms are, of course, included as well as others which may have more significance as the number of types of electroluminescent crystals increases.

Electroluminescence is the excitation of luminescence as a result of the existence of an applied potential difference in the phosphor material. The definition includes luminescence induced by any mechanism of injection of electrons or holes into the phosphor or any mechanism of creating free charge carriers in the phosphor if the energy of the emitted radiation originates in the electric potential difference applied to the phosphor. Cathodoluminescence is excluded since in this case the excitation energy is supplied initially to electrons by an external field.

It is well known that solid-state luminescence usually originates from excited impurity systems called activators which have dimensions of the order of an interatomic distance. To radiate in the visible portion of the spectrum, the activator system must have an excited state at least 2 ev higher than the ground state. An electroluminescent mechanism utilizing an activator system must in some way localize 2 or 3 ev of the energy available in the applied potential to the atomic dimensions of the activator system and transfer this energy to the activator. If the activator is left in an excited state, it is then able to radiate a photon in returning to the ground state. Ionization of the center is also a permissible mechanism, provided conduction electrons are available or are made available subsequently.

The most straightforward mechanism of electroluminescent excitation is direct field ionization of the activator system. Since the ionized state of the activator system is at least 2 ev above the ground state, the field strength necessary to ionize these centers at a reasonable rate would normally be in excess of the dielectric breakdown strength of the crystalline matrix. Breakdown in materials with suitable band gaps for luminescence normally occurs by an avalanche mechanism, rather than by field ionization of the valence electrons. Nevertheless, direct field ionization of the activator system

[1] O. Lossev, Phil. Mag. **6**, 1024 (1928).
[2] G. Destriau, Phil. Mag. **38**, 700 (1947).
[3] Lehovec, Accardo, and Jamgochian, Phys. Rev. **83**, 603 (1951).
[4] Payne, Mager, and Jerome, Illum. Eng. **45**, 688 (1950).
[5] W. W. Piper and F. E. Williams, Phys. Rev. **87**, 151 (1952); Brit. J. Appl. Phys., Supplement No. 4, **6**, 39 (1955).
[6] D. Curie, J. phys. radium **13**, 317 (1952).
[7] J. F. Waymouth and F. Bitter, Phys. Rev. **95**, 941 (1954).
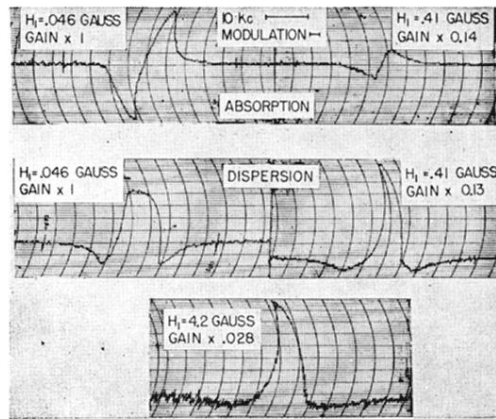
FIG. 2. Absorption and dispersion signals in pure aluminum at various rf power levels. The modulation was 14~ in phase with the lock-in detector and the resonance frequency was about 7.6 megacycles per second.
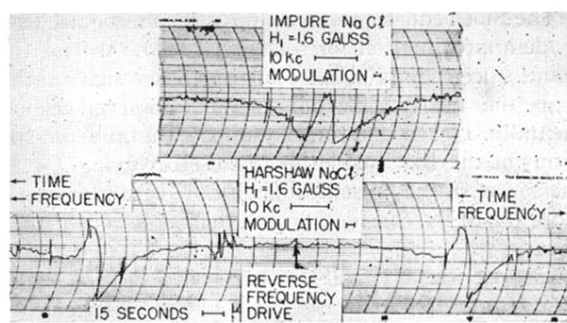
FIG. 5. Apparent dispersion derivatives in samples of NaCl of different purity. The Na[23] nucleus was observed at a frequency of about 7.5 megacycles. The modulation frequency was 41 cps in phase with the lock-in detector.